TÉCNICO LISBOA

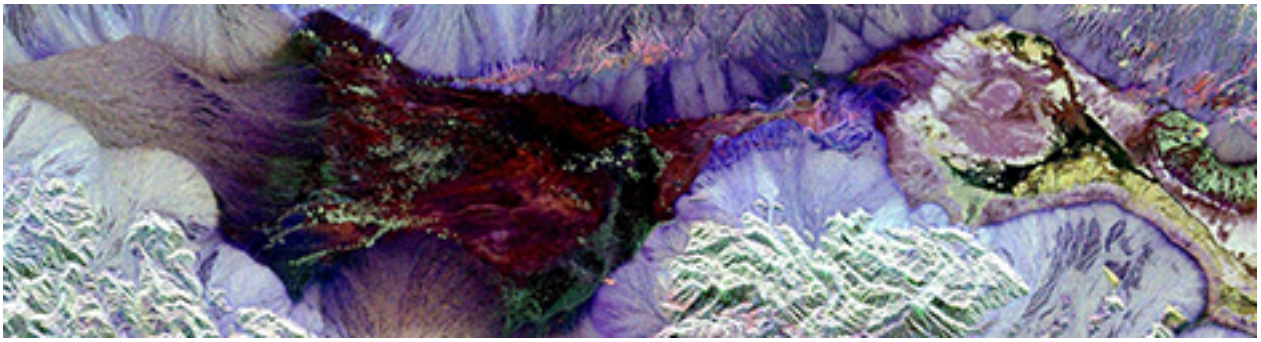

Synthetic Aperture Radar Imagery Analysis and Applications Using SOCET GXP®

Afonso Roque Rodrigues Martins Duarte

Thesis to obtain the Master of Science Degree in

Electrical and Computer Engineering

Supervisor: Prof. António Luís Campos da Silva Topa

Examination Committee

Chairperson: Prof. José Eduardo Charters Ribeiro da Cunha Sanguino
Supervisor: Prof. António Luís Campos da Silva Topa
Member of the Committee: Prof. António José Castelo Branco Rodrigues

May 2021

I declare that this document is an original work of my own authorship and that it fulfills all the requirements of the Code of Conduct and Good Practices of the Universidade de Lisboa.

Acknowledgments

The completion of this project represents the culmination of a wide chain of events of various forms and flavours. Primarily, I would like thank God for being able to complete this project with success. I would also like to thank my parents for their friendship, caring over all these years and for always being the first ones to tell me to push further and beyond. The same goes for my grandparents and extended family for always being there for me through thick and thin and without whom this project would not have come to fruition and, of course, to all my friends and colleagues that made my life not easier, but harder. I hereby express my gratitude to my dissertation supervisor Prof. António Topa for all his insight, patience and for bringing me the opportunity to face this endeavour. Finally, I would also like to give my special thanks to Jay Gordon and Diego Balcázar over at BAE SYSTEMS for taking the time to provide me with vital information and, most importantly, for giving me the opportunity to use SOCET GXP® for the purposes of this dissertation without which it would not be possible. This dissertation had as its host institution, the Telecommunications Institute (Instituto de Telecomunicações).

Abstract

Synthetic Aperture Radar (SAR) has been extensively used for remote sensing of the Earth for a few decades. It provides high resolution images in an all weather, day and night fashion for a multitude of applications. With the advances in RADAR technology, more and more data is generated and needs to be analysed and processed. The main purpose of this dissertation is to provide a reader who is interested in SAR imagery a good starting point to get accustomed to application oriented SAR data processing and visualization. This goal is achieved using BAE SYSTEMS SOCET GXP® software tool. The document provides the reader with key SAR concepts (imaging modes, product levels, polarisations, etc) followed by various simulations of some of the tool's features in real world applications as well as several use cases. The obtained results present a solid approach to the novice analyst by using the tool for the exploitation of SAR images as a source for geospatial information and data regarding water resource detection, terrain feature extraction, vegetation health assessment among other applications.

Keywords

Synthetic Aperture Radar, Image Processing, Image Visualization, Feature Extraction, Geospatial Products, BAE SYSTEMS SOCET GXP®

Resumo

O Radar de Abertura Sintética (SAR) tem sido amplamente utilizado para o mapeamento remoto da Terra há algumas décadas. Fornece imagens de alta resolução em todas as condições climatéricas, de dia e de noite, para uma vasta gama de aplicações. Com os avanços da tecnologia de RADAR, cada vez mais dados são gerados e precisam de ser analisados e processados. O principal objetivo desta dissertação é fornecer ao leitor interessado em imagens SAR um bom ponto de partida para iniciar o processamento e a visualização de dados SAR orientados a usos específicos. Este objetivo é alcançado utilizando a ferramenta de software da BAE SYSTEMS, SOCET GXP®. Este documento apresenta ao leitor os principais conceitos de SAR (modos de imagem, níveis de produto, polarizações, etc.) seguido de várias simulações envolvendo algumas das potencialidades da ferramenta em aplicações do mundo real, bem como certos casos de utilização. Os resultados obtidos apresentam uma abordagem consistente para o analista iniciante usando a ferramenta para a exploração de imagens SAR como uma fonte de informações geoespaciais e dados relativos à detecção de fontes de água, extração de características de terreno, avaliação da saúde de vegetação entre outras aplicações.

Palavras Chave

Radar de Abertura Sintética, Processamento de Imagem, Visualização de Imagem, Extração de Características, Produtos Geoespaciais, BAE SYSTEMS SOCET GXP®

Contents

1 Introduction **1**

1.1 Motivation . . . 3
1.2 Topic Overview . . . 4
1.3 Objectives . . . 4
1.4 Dissertation Outline . . . 5
1.5 Main Contributions . . . 5

2 Scientific Outlook **7**

2.1 The Radar Equation . . . 9
2.2 Noise Power . . . 10
2.3 Signal-to-Noise Ratio (SNR) . . . 10
2.4 Radar Cross Section (RCS) . . . 11
2.5 SAR State of the Art . . . 11
2.5.1 Real and Synthetic Aperture . . . 12
2.5.2 Range Resolution . . . 13
2.5.3 Crossrange Resolution . . . 14
2.6 Calibration . . . 14
2.6.1 Radiometric Calibration . . . 15
2.6.2 Geolocation Accuracy . . . 16
2.6.3 Synthetic Aperture Focusing Calibration . . . 17
2.7 Data Acquisition . . . 17
2.8 Data Processing . . . 18
2.9 Probes and Sensors . . . 19
2.10 Challenges . . . 20
2.10.1 Optimum Frequency Band . . . 20
2.10.2 Signal to Clutter in Rain . . . 20
2.10.3 Pulse Management . . . 20
2.10.4 Range Extension . . . 21

3 Imagery **23**
3.1 Bands of Operation . . . 25
3.2 Signal Polarization and Scattering . . . 26
3.2.1 Superficial and Volume Scattering . . . 26
3.2.2 ”Double Bounce” or Multipath Scattering . . . 27
3.3 Speckle . . . 28
3.4 Geometric Distortion . . . 29
3.5 Imaging Modes . . . 30
3.5.1 Stripmap Imaging Mode . . . 30
3.5.2 Spotlight Imaging Mode . . . 31
3.5.3 ScanSAR Imaging Mode . . . 31
3.6 SAR Products . . . 32
3.6.1 Level-0 Products . . . 32
3.6.2 Level-1 Products . . . 33
3.6.2.A Level-1 Single Look Complex (SLC) Products . . . 33
3.6.2.B Level-1 Ground Range Detected (GRD) Products . . . 34
3.6.3 Level-2 Geocoded Products . . . 34
3.6.4 Level-3 and Level-4 Products . . . 34
3.7 Rules of Thumb for SAR Image Interpretation . . . 34
3.8 Available Tools . . . 35
3.8.1 PolSARpro (Biomass Edition) Toolbox . . . 35
3.8.2 ASF MapReady . . . 36
3.8.3 ENVI™ SARscape . . . 36
3.8.4 BAE SYSTEMS SOCET GXP® . . . 36
3.9 SOCET GXP® Tool Characterization . . . 37
3.10 Context . . . 38
4 SAR Tool Capabilities **39**
4.1 Data Limitations . . . 41
4.2 In-Software Approach . . . 41
4.3 Histogram Features . . . 43
4.4 Threshold LUT . . . 44
4.5 Width and Height Measurements . . . 44
4.6 Multi-Spectral Imagery Classification . . . 45
4.7 Spectral Angle Mapper . . . 46
4.8 Colorization . . . 47

5 Use Cases **49**
5.1 Foreword . . . 51
5.2 Soil Moisture Estimation . . . 51
5.3 Subsidence Estimation . . . 52
5.4 Forest Height Estimation . . . 53
5.5 Oil Spill Detection . . . 55
6 Conclusion **57**
6.1 Overview . . . 59
6.2 Future Work . . . 60
6.2.1 Data Availability . . . 60
6.2.2 Advanced Imaging Techniques . . . 61
6.3 Final Remarks . . . 61

List of Figures

1.1 Airborne SAR Imaging [1]. . . . 3
1.2 SAR image of Death Valley colored using polarimetry [2]. . . . 4

2.1 Example of an antenna on a moving platform [3]. . . . 12
2.2 Diagram of a real aperture antenna [4]. . . . 13
2.3 Diagram of a synthetic aperture antenna [4]. . . . 13
2.4 Range, crossrange and slant on a 3D plane [5]. . . . 14
2.5 The SAR product formation chain. . . . 17
2.6 Example of a TerraSAR-X High Resolution Image (Panama Channel). . . . 20

3.1 Sensitivity of SAR measurements to forest environment and depth of vegetation penetration at different wavelengths [6]. . . . 25
3.2 Scattering types in a real world scenario [6]. . . . 26
3.3 Double bounce scattering in different scenarios [7]. . . . 27
3.4 A before (top) and after (bottom) speckle reduction comparison of a RADAR image [8]. . . . 28
3.5 Geometric distortion types [7]. . . . 29
3.6 Illustration of the Stripmap SAR Imaging Mode [9]. . . . 30
3.7 Illustration of the Spotlight SAR Imaging Mode [9]. . . . 31
3.8 Illustration of the ScanSAR Imaging Mode [9]. . . . 32
3.9 High-resolution image of the Panama Canal from sample data using SOCET GXP®. . . . 38

4.1 Slant (left) and ground (right) plane visualization rendered from sample data using SOCET GXP® (Lake Constance, Germany). . . . 42
4.2 SAR Overlay enabled using SOCET GXP®. . . . 42
4.3 Image histogram using SOCET GXP®. . . . 43
4.4 Threshold values at: 0 (left), 50 (center), 99 (right) using SOCET GXP® (Lake Constance, Germany). . . . 44
4.5 Farmland plot width measurement using SOCET GXP® (Lake Constance, Germany). . . . 45

4.6 Building height measurement using SOCET GXP® (Rio de Janeiro, Brazil). 45
4.7 Band filtering with near-infrared selection at 833 nm wavelength using SOCET GXP® (Rio de Janeiro, Brazil). 46
4.8 Supervised classification of vegetation, roads and water using SOCET GXP® (Tripoli, Libia). 46
4.9 Water resource detection through colorization using SOCET GXP® (Lake Constance, Germany). 47

5.1 Soil moisture maps obtained after applying polarimetric decomposition to remove the vegetation layer and inverting the remaining ground component [10]. 52
5.2 (a) Estimated subsidence over Mexico City obtained with two TerraSAR-X images acquired with a 6 month difference (overlay of reflectivity and phase) (b) Mean deformation velocity estimated over Mexico City (c) Zoom over the city of the refined DEM retrieved as an additional product to the deformation velocity, where the individual buildings can be observed. The scene size is approximately 8 km x 8 km. RADAR illumination from the right [10]. 53
5.3 (a) L-band HV intensity image of the Traunstein test site. Forest height map computed from Pol-InSAR data in (b) 2003 and (c) 2008 [10]. 54
5.4 Original oil spill SAR image (left) and post-classification SAR image (right) [11]. 55

List of Tables

3.1 SAR Bands of Operation. 25

List of Symbols

β_0	Observed RADAR brightness
$\Delta\theta$	Synthetic aperture angle as seen from the target area
δ_{cr}	Crossrange (azimuth) resolution
δ_r	Range resolution
λ	Wavelength
Ψ	Grazing angle at target location
σ	Target Radar Cross Section
σ_0	Target reflectivity
θ_B	Antenna aperture
θ_{loc}	Local incidence angle of the scattering area
A_e	Receiver antenna effective area
B	Bandwidth
B_W	Equivalent noise bandwidth
c	Speed of light in a vacuum
D	Antenna diameter
DV	Digital value of the pixel value
F_n	Receiver noise figure
G_A	Transmitter antenna gain factor
G_r	SNR gain due to range processing (range compression)

G_α SNR gain due to crossrange processing (azimuth compression)

I Inphase component of the complex image pixel

k Boltzmann constant

k_s Calibration factor provided in the image metadata

L_{atmos} Atmospheric loss factor

L_{radar} Transmission loss factor due to miscellaneous sources

L_{SA} Synthetic aperture length

L_{sp} SNR loss due to a variety of signal processing issues

NEB Noise floor of the RADAR system in terms of observed RADAR brightness β_0

NES Noise equivalent sigma

P_r Received signal power

P_t Transmitter signal power

Q Quadrature component of the complex image pixel

R Range

r_s Range vector from target to the antenna

T Time

T_0 Nominal noise temperature

V Platform speed

Acronyms

CCD	Coherent Change Detection
DEM	Digital Elevation Model
GRD	Ground Range Detected
ISP	Instrument Source Packets
LOS	Line of Sight
LUT	Look Up Tables
MSI	Multi-Spectral Imagery
RCS	Radar Cross Section
RADAR	Radio Detection And Ranging
RAR	Real Aperture Radar
SICD	Sensor Independent Complex Data
SNR	Signal-to-Noise Ratio
SLC	Single Look Complex
SAR	Synthetic Aperture Radar
UAV	Uninhabited Aerial Vehicle

1

Introduction

Contents

1.1 Motivation 3
1.2 Topic Overview 4
1.3 Objectives 4
1.4 Dissertation Outline 5
1.5 Main Contributions 5

1.1 Motivation

If one was asked to condense in a single word what Electrical Engineering is all about, Radio Detection And Ranging (RADAR) would probably be a very good candidate. Its composition involves all the intricate parts that make up an engineering student's career such as signal processing, electromagnetism, microwaves and so forth. But when it comes to the real world, these are merely sub parts of some type of system that actually possesses an actual, useful application. And here is where RADAR comes into play.

When we mention to RADAR we are usually referring to a Real Aperture Radar (RAR) where the antenna is a physical object that first emits, and then collects, radiation. In this particular case we are going to be covering Synthetic Aperture Radar (SAR) systems where the antenna is in motion in order to cover a synthetic aperture, hence its designation and acronym. These systems possess a diverse quiver of applications such as remote sensing, surface mapping and foliage penetration.

By taking a brief look at this short list, one can without difficulty think of a multitude of applications where SAR might be applied. Ranging from topography and oceanography to monitoring infrastructure stability and even military surveillance, the opportunities are virtually endless making this specific topic one of the utmost importance to explore. The aim is to explore several solutions involving the use of SAR systems and specifically data processing and visualization tools.

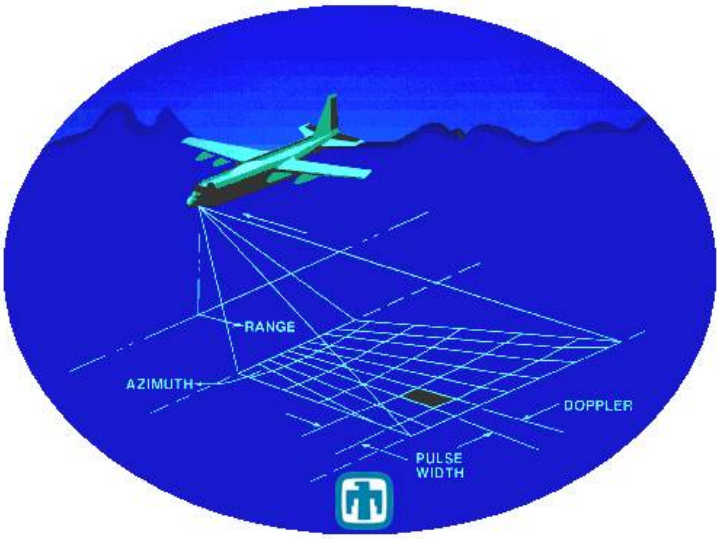

Figure 1.1: Airborne SAR Imaging [1].

1.2 Topic Overview

Applications such as environmental monitoring, earth-resource mapping, and military systems require broad-area imaging at high resolutions. And as is the case with RADAR, SAR systems' performance revolves around the correct (and sometimes lucky) alignment of a multitude of parameters that are often correlated in a non-linear fashion. These parameters concern not only technology constraints but mostly aspects that are not necessarily under human control such as weather conditions and other physical atmospheric phenomena.

This technique provides high resolution with the remarkable characteristic that its resolution does not degrade with distance. Distance weakens the strength of the RADAR reflections and can increase image noise, but resolution cell size does not increase as distance increases.

Other advantages of working with SAR technology include the ability to extract different features from different bands of operation at which one collects data from a specific physical location. Consequently, this action will result in heavy amounts of SAR data in more or less fine resolutions. Independently of what the case may be, a few options are available referring to what tools can one use to visualize, analyze and process the vast amount of data that can be collected by any probe or sensor. This will be the main focus of this work.

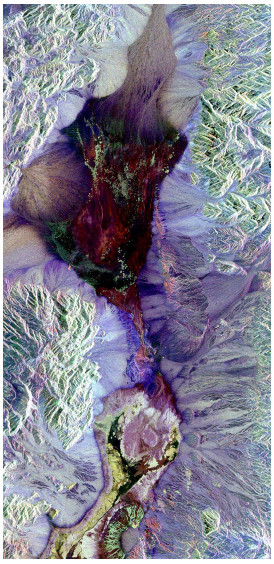

Figure 1.2: SAR image of Death Valley colored using polarimetry [2].

1.3 Objectives

It is certain that SAR technology has much to offer. With several satellite constellations already in operation as well as multiple airborne sensors, there is plenty of data to be processed and analysed.

With this notion in mind, several software tools were considered (both personal and commercial) and eventually one was chosen to tackle the task.

Ultimately, we will be addressing the chosen software solution in an attempt to expose the capabilities of such tool as well as the kind of information that can be extracted using it when working with SAR imagery from any kind of source. A few use cases will also be presented with the intent of providing a good starting point for anyone interested in beginning to work with SAR data, particularly when it comes to processing, visualization and feature extraction.

1.4 Dissertation Outline

This document is organized as follows: in chapter 2 a brief scientific background regarding RADAR is given from a physics and electromagnetics standpoint addressing relevant concepts to bear in mind before moving on to SAR specific concepts and particularities. Several examples of probes and sensors are also given as well as known challenges when working with RADAR imaging.

In chapter 3 we delve into SAR imagery going over essential concepts such as bands of operation, polarization and product types. This chapter is meant to provide the reader with relevant, foundational information that will enable a more knowledgeable approach further on when the actual tools are presented and selected. Said tools are then discussed in regards to its specific features. SOCET GXP® capabilities pertaining specifically to SAR imagery analysis are addressed in chapter 4.

In chapter 5 a few use cases will be explored where several real-world scenarios are taken into account such as dealing with differently polarized data, location specific data and how the overall dataset characteristics impact the features that can be extracted and the conclusions to be drawn. Moreover, how such data can enable certain key SAR capabilities is also addressed.

Finally, in chapter 6 a reflection is made revolving around what was achieved in the analysis realm, what wasn't and why was that the case. Some considerations are also made in regards to future work in the field of SAR imagery processing and visualization tools.

1.5 Main Contributions

The major contribution of this dissertation lies in providing the novice reader looking into SAR imagery processing and visualization a comprehensive systematization of the fundamental concepts needed to venture further into the world of geospatial products. This work fills a major gap present in the literature regarding SAR imagery analysis and the available tools to do so. It does not prevent the reader from advancing his/her research by not assuming the knowledge of certain concepts inherent to SAR imagery, of the tools to process such imagery and of how results are obtained for real world scenarios.

2

Scientific Outlook

Contents

2.1 The Radar Equation 9
2.2 Noise Power 10
2.3 Signal-to-Noise Ratio (SNR) 10
2.4 Radar Cross Section (RCS) 11
2.5 SAR State of the Art 11
2.6 Calibration 14
2.7 Data Acquisition 17
2.8 Data Processing 18
2.9 Probes and Sensors 19
2.10 Challenges 20

A RADAR is an sensor which is sensible enough to detect and locate electromagnetic waves which are reflected by other objects. Firstly, it radiates energy in the form of electromagnetic waves from an antenna which then propagate in a given medium. Secondly, some of this radiated energy collides with a reflecting object, which is usually called a *target*, and is located at a certain distance from the RADAR. Next, as this energy collides with the target, it is re-radiated in multiple directions. Some of these directions happens to be the one of the receiver antenna and is perceived as echo. Finally, through amplification and adequate signal processing, a decision is made at the output of the receiver as to whether or not a target echo signal is present and allows us to determine the target location as well as some other useful information. [12]

2.1 The Radar Equation

We can now translate these parameters such as radiated and received energy into measurable entities and establish a relation between them. With this purpose in mind, it is now time to bring up the famous and governing, Radar Range Equation, widely known as simply Radar Equation. With it, it is possible not only to compute an estimate of the range of a certain system as a function of its characteristics but also to use it as a great starting point for designing a RADAR system:

$$P_r = P_t G_A (\frac{1}{4\pi |r_s|^2}) \sigma (\frac{1}{4\pi |r_s|^2}) A_e \tag{2.1}$$

which becomes:

$$P_r = \frac{P_t G_A A_e \sigma}{(4\pi)^2 |r_s|^4 L_{radar} L_{atmos}} \tag{2.2}$$

- $P_r =$ Received signal power (W)
- $P_t =$ Transmitter signal power (W)
- $G_A =$ Transmitter antenna gain factor
- $A_e =$ Receiver antenna effective area (m^2)
- $\sigma =$ Target Radar Cross Section (RCS) (m)
- $r_s =$ Range vector from target to the antenna (m)
- $L_{radar} =$ Transmission loss factor due to miscellaneous sources
- $L_{atmos} =$ Atmospheric loss factor

2.2 Noise Power

Target detection in a binary form is of little value if we cannot obtain some other information in regards to it. Then again, target information without detection is also meaningless and thus, besides range, we can also obtain information relating to radial velocity, angular direction, a target's size and shape, and of course, the Signal-to-Noise Ratio (SNR) which is the absolute indicator of all RADAR measurements. Since we are dealing with a real world scenario there are many factors which are not considered in the Radar Equation rendering it useless unless we take into account relevant modifications. The received signal at the antenna is constantly competing with noise from miscellaneous sources such as air pressure, smoke, weather conditions, etc. This noise power, or the minimum signal power that can be detected, can be expressed as:

$$S_{min} = kT_0B_WF_n \tag{2.3}$$

where:

- $k =$ Boltzmann Constant
- $T_0 =$ Nominal noise temperature
- $B_W =$ Equivalent noise bandwidth
- $F_n =$ Receiver noise figure

2.3 Signal-to-Noise Ratio (SNR)

For a received signal to be detected, it must be larger than the receiver noise by a factor denoted by the Signal-to-Noise Ratio as mentioned before:

$$SNR_{antenna} = \frac{P_r}{N_r} = \frac{P_tG_AA_e\sigma}{(4\pi)^2|r_s|^4L_{RADAR}L_{atmos}S_{min}} \tag{2.4}$$

Signal processing gains and losses must be taken into account:

$$SNR_{image} = SNR_{antenna}(\frac{G_rG_a}{L_{sp}}) = \frac{P_tG_AA_e\sigma G_rG_a}{(4\pi)^2|r_s|^4L_{RADAR}L_{atmos}L_{sp}S_{min}} \tag{2.5}$$

where:

- $G_r =$ SNR gain due to range processing (range compression)
- $G_a =$ SNR gain due to crossrange processing (azimuth compression)
- $L_{sp} =$ SNR loss due to a variety of signal processing issues

2.4 Radar Cross Section (RCS)

The Radar Cross Section of a given target literally reflects its ability to transmit energy back to the RADAR. For the specific case of SAR systems, the target of interest in terms of RADAR performance is generally a widespread, distributed target, such as plain fields with open areas, areas with dense foliage and vegetation or even metropolitan environments. Of course, for this target type, the RCS is dependent on the area being scanned and processed. Thus, for distributed targets, it is useful to specify RCS in terms of a 'reflectivity' unit that quantifies RCS per unit area and so, the actual area is the area of a resolution cell, as projected on the ground:

$$\sigma = \sigma_0 \delta_{cr} (\frac{\delta_r}{cos\Psi}) \tag{2.6}$$

where:

- $\sigma_0 =$ Target reflectivity (m^2/m^2)
- $\delta_{cr} =$ Crossrange resolution (m)
- $\delta_r =$ Range resolution (m)
- $\Psi =$ Grazing angle at target location

This cross section is likely to share a dependency with the SAR's working frequency, the grazing angle and the target's overall shape (grass, trees, buildings, roads, etc).

At this point we are now able to examine SNR terms and factors individually and establish relations between them and physical SAR system parameters with performance criteria in mind.

2.5 SAR State of the Art

As mentioned before, and unlike regular RADAR systems, SAR systems allow us to acquire imagery in the most challenging of circumstances and scenarios such as at night or under harsh atmospheric conditions. The aim is always to achieve a finer resolution whether we are airborne or spaceborne. Thanks to SAR, we can now take advantage of the long-range propagation characteristics of RADAR signals and the complex information processing capability of modern digital electronics to provide high resolution imagery.

SAR systems produce two-dimensional (2D) images, one dimension being *range* or the resolution along the line-of-sight Line of Sight (LOS) from the RADAR to the target region and the second dimension being the *crossrange* (or azimuth) resolution or the resolution along the direction perpendicular to the LOS and parallel to the ground [1]. Refer to Figure 2.4 for a more helpful illustration.

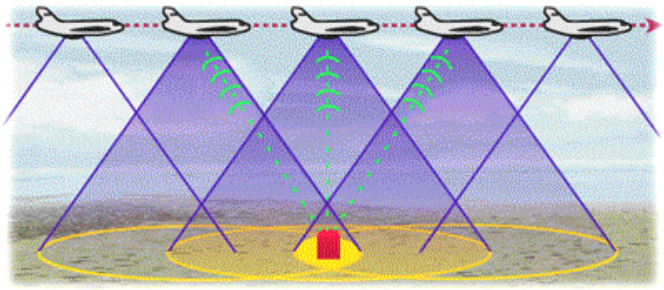

Figure 2.1: Example of an antenna on a moving platform [3].

SAR's ability to produce relatively fine azimuth resolution makes it stand out from the crowd. Usually, to obtain fine crossrange resolution, a physically large antenna is needed to focus the transmitted and received energy into a sharp beam. The sharpness of the beam defines the crossrange resolution. Likewise, optical systems, such as telescopes, require large apertures (mirrors or lenses which are analogous to the RADAR antenna) to obtain fine imaging resolution. Since SAR uses much lower frequencies than optical systems, even moderate resolutions require an impractically large antenna to be carried by an airborne platform: antenna lengths of several hundred meters long are often required. However, airborne RADAR can collect data while flying this distance, and then process the data as if it came from a physically long antenna. [13]

The distance the aircraft flies in synthesizing the antenna is known as the synthetic aperture (see fig. 2.1). A narrow synthetic beam width results from the relatively long *synthetic* aperture, which yields finer resolution than is possible from a smaller physical antenna. [4]

2.5.1 Real and Synthetic Aperture

Crossrange resolution was initially achieved using a narrow beam. Its width in radians of an aperture antenna is given approximately by the wavelength divided by the aperture diameter. The corresponding linear crossrange resolution at range R is then:

$$\delta_{cr} \approx \frac{R\lambda}{D} \tag{2.7}$$

or, in other words, a *real aperture.*

Now, if we move the platform of this physical antenna along a path in space we would, in principle, be able to achieve a crossrange resolution comparable to what would be achieved in a scenario where a real aperture antenna would have a length equal to the path length, thus making it a *synthetic aperture*, L_{SA}:

$$\delta_{cr} \approx \frac{R\lambda}{2L_{SA}} \approx \frac{\lambda}{2\Delta\theta} \tag{2.8}$$

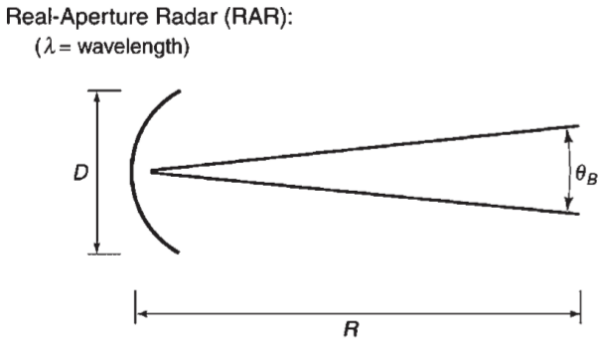

Figure 2.2: Diagram of a real aperture antenna [4].

where $\Delta\theta$ is the synthetic aperture angle, as seen from the target area. The additional factor of 2 occurs due to signal processing. For figures 2.2 and 2.3, $\theta_B = \frac{\lambda}{D}$.

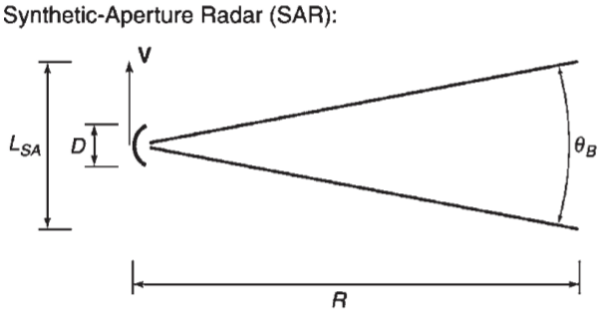

Figure 2.3: Diagram of a synthetic aperture antenna [4].

2.5.2 Range Resolution

Range provides an indication of the size of the smallest object identifiable in a particular acquired image. When it comes to *range resolution*, and in order to introduce the concept in an simpler way, we will resort to a step-frequency waveform which consists on a train of identical pulses of width τ. The phase and amplitude of each pulse echo is intercepted by the RADAR. After application of several Fourier Transforms, and noting that each pulse has a width of $1/B$ (bandwidth B) and the same for the sampling time interval:

$$\delta_r = \frac{c}{2B} \tag{2.9}$$

with the multiplication by $c/2$ since an incremental delay Δt corresponds to an incremental downrange distance of $c\Delta t/2$. The resolution is thus given in terms of pixel separation. [14]

2.5.3 Crossrange Resolution

Crossrange resolution, or *azimuth*, corresponds to the resolution along the direction perpendicular to the LOS and parallel to the ground and increases with range. If we assume that the SAR is moving at a constant altitude H, speed V and time T along a direction perpendicular to the LOS we can state that $L_{sa} = VT$ and very small in comparison with the range R to the target area. With this taken in due consideration, and using eq. (2.8):

$$\delta_{cr} = \frac{\lambda}{2\Delta\theta} \approx \frac{\lambda R}{2L_{SA}} = \frac{\lambda R}{2VT} \tag{2.10}$$

In fig. 2.4 we can see in relevant detail the relationship between these parameters.

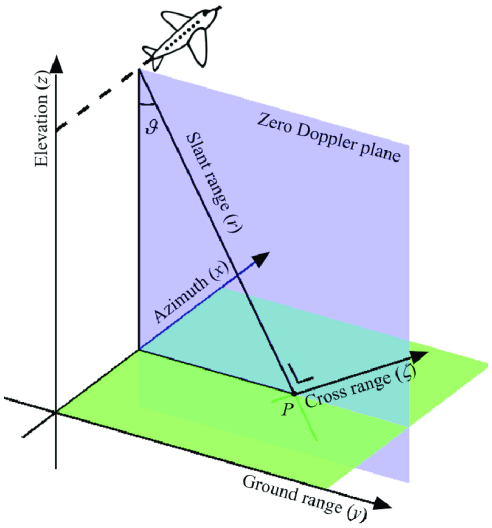

Figure 2.4: Range, crossrange and slant on a 3D plane [5].

2.6 Calibration

A key strength of SAR is that it is also a precise measuring instrument as a well as a mapping tool. It is therefore possible to obtain RADAR reflective properties from the scene by analysing the digital values within the SAR image. To achieve this, the imbalances and dispersions within the RADAR and SAR processor have to be accounted for. This is the purpose of calibration and will be covered in this subsection. Usually, satellites use a range of calibration sites around the world as well as internal closed loop calibration checks performed during the engineering and manufacturing process.

2.6.1 Radiometric Calibration

Radiometric calibration is required to associate the digital values within a SAR image with the mean RADAR cross section σ (also known as the backscatter coefficient) in m^2/m^2. The calibration compensates for effects due to:

- The atmosphere (delay and oscillations of the signal during tropospheric and ionospheric propagation)
- The antenna (distribution of radiated energy in range and azimuth)
- The electronic instrument (variation of transmitted power and receiver gain)
- The processor (contributions due to the implemented SAR image formation algorithm)

An area of the ground with a given backscatter coefficient σ in a SAR product will have a different observed brightness (and hence different digital value in the SAR image) when the terrain is angled towards the sensor. This can be computed from:

$$\sigma = \beta_0 \sin \theta_{loc} - NES \tag{2.11}$$

where:

- β_0 - Observed RADAR brightness
- θ_{loc} - Local incidence angle of the scattering area
- NES - Noise equivalent sigma

It is important to note that the noise equivalent sigma represents the noise component that inherently exists within the pixel in terms of a mean RADAR backscattering coefficient. β_0 can be obtained from:

$$\beta_0 = k_s |DV|^2 \tag{2.12}$$

where:

- k_s - Calibration factor provided in the image metadata
- DV - Digital value of the pixel value

Furthermore, the digital value, DV, is given by:

$$|DV|^2 = I^2 + Q^2 \tag{2.13}$$

where:

- I - Inphase component of the complex image pixel

- Q - Quadrature component of the complex image pixel

Finding the noise component NES is the primary purpose of calibration. The NES value however is also a function of range and the local incidence angle and so can be considered in terms of a minimum RADAR brightness β_0 as:

$$NES = NEB \sin \theta_{loc} \tag{2.14}$$

where:

- NEB - Noise floor of the RADAR system in terms of observed RADAR brightness β_0

The backscatter coefficient for a SAR pixel is therefore provided by:

$$\sigma = (k_s \cdot |DV|^2 - NEB) \sin \theta_{loc} \tag{2.15}$$

During early deployment stages and periodically during missions operations, the satellite constellations perform routine collections over areas of the world that have well characterised isotropic scattering, typically the Amazon Rainforest and The Congo. [9] Beam calibration then provides a measure for system noise as a function of beam angle which are applied as corrections to digital values in level 1 image products using an ellipsoid model (addressed further in section 3.6) to determine $\theta_{loc} \cdot \sigma$ can therefore be directly computed from the image product by:

$$\sigma = k_s \cdot |DV_{corrected}|^2 \tag{2.16}$$

2.6.2 Geolocation Accuracy

Geolocation accuracy is the error associated with the location of a scattering object within a pixel in a SAR image compared to the object's true location. Errors in geolocation accuracy are primarily due to the precision with which the satellite's location is known and is related to the precision that the satellite's orbit can be tracked. Usually, its orbits are tracked using GPS acquisitions prior to an imaging operation. These are downloaded with the raw image data and refined during the processing stage. To validate the geolocation accuracy of SAR products, corner reflectors, situated at calibration sites around the world are used. Each corner reflector's location is precisely known in 3D space.

2.6.3 Synthetic Aperture Focusing Calibration

Calibration of the SAR image formation processor's focusing ability is also performed using calibration target situated at ground level sites. Corner reflectors are used as they act as point targets within a pixel. The point target's impulse response function can then be measured and compared to the theoretical best performance. Degradation of focusing manifests itself in raised sidelobe levels and so these are provided as a measure of performance.

2.7 Data Acquisition

At each crossrange position along a certain trajectory, the moving SAR broadcasts pulses and is aware of the respective echoes. This information is then stored in the shape of a two-dimensional array of complex numbers consisting of magnitude and phase (see fig. 2.5 for the data flow). If we process this data as a function of downrange and crossrange it is possible to render a RADAR image.

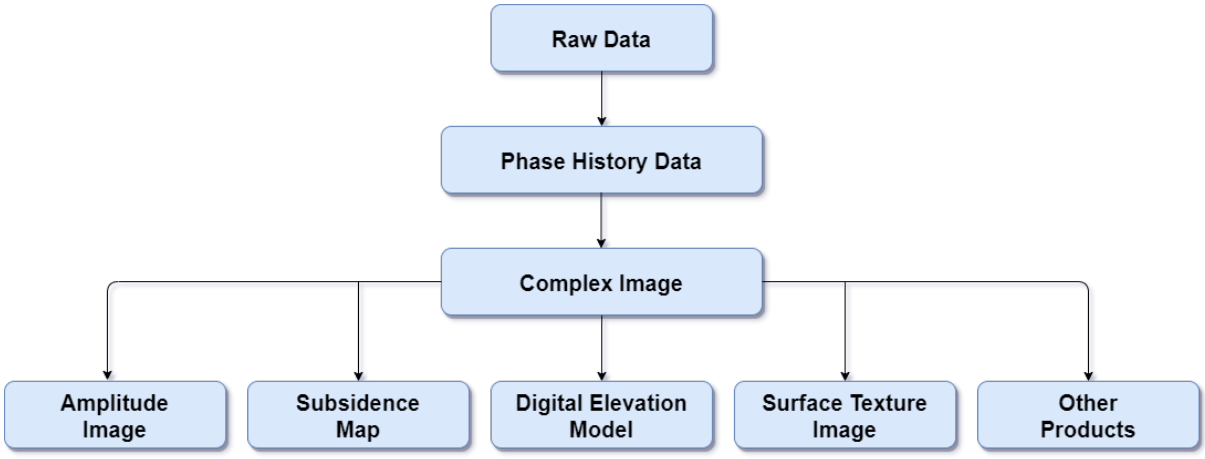

Figure 2.5: The SAR product formation chain.

The acquisition system can be defined through the following three frequencies.

The first one corresponds to the oscillator frequency (f_c) (the RADAR's carrier frequency, defining the wavelength):

$$\lambda = \frac{c}{f_c} \tag{2.17}$$

The second one defines the length of a range pixel through the sampling frequency. As the RADAR measures slant range, the ground range pixel is the projection of the slant range pixel on the ground. For the echo of a pulse to be sufficiently sampled, f_d must be larger than the pulse modulation bandwidth (which determines the instrument resolution). The range resolution of the acquired data is thus finer than

the instrument resolution:

$$p_d = \frac{c}{2f_d} \tag{2.18}$$

Finally, and no less relevant, the third frequency pertains to pulse repetition (f_a) which, along with the SAR's velocity v, will dictate the crossrange (or azimuth) resolution of the acquired data. In other words, the length of a crossrange pixel:

$$p_a = \frac{v}{f_a} \tag{2.19}$$

With these parameters in mind, we are now ready to begin processing this data and address the aforementioned topics on section 2.3 regarding compression. [14]

2.8 Data Processing

The conversion of return delay time to geometric range can be very accurate because of the natural, unchanging speed and direction of propagation of electromagnetic waves. Obtaining high-resolution images involves three-dimensional processing which is comprised of two stages: range and azimuth compression.

Next, a Digital Elevation Model (DEM) is used to measure the phase differences between the acquired complex arrays, which is determined from different acquisition angles to discern the height information. This height information, along with the crossrange coordinates provided by two-dimensional SAR focusing, will provide the third dimension, which is elevation. The reflected signal that is captured by the receiving antenna is a significantly lower, attenuated power and time-shifted version of the original signal, the latter being our reference signal.

While performing *range compression*, the received signal is correlated with the reference signal with the result being the information on the target's range. This is also referred to as a *matched filter* which consists in the application of a Fast Fourier Transform to both signals, multiplying the two and then performing a reverse transform on this product. If the antenna possesses a wide crossrange beam width, the received signals may sometimes be recorded in several range "bins" which can also be described in terms of range resolution cells. This will cause the "perceived" trajectories to be shifted and so, for a single target, they will all fit the same range bin for the entirety of the synthetic aperture.

Finally, crossrange compression is applied also using a *matched filter*, but performed in the azimuth direction for each range bin. [14]

Compression is of the utmost importance since an aircraft flies through a non-uniform atmosphere, and the relating of pulse transmission and reception times to successive geometric positions of the antenna must be accompanied by constant adjusting of the return phases to account for irregularities in the flight path.

The interpretation of SAR images is not straightforward but a few rules of thumb can be made for example: regions of calm water and other smooth surfaces appear black and rough surfaces appear brighter, as they reflect the RADAR in all directions, and more of the energy is scattered back to the antenna. A rough surface backscatters even more brightly when it is wet. Hills and other large-scale surface variations tend to appear bright on one side and dim on the other and so, the side that appears bright was facing the SAR. Due to the reflectivity and angular structure of buildings, bridges, and other human-made objects, these targets tend to behave as corner reflectors and show up as bright spots in a SAR image, a particularly strong response.

2.9 Probes and Sensors

At the time of writing, organizations such as NASA's Jet Propulsion Laboratory, the European Space Agency and AIRBUS are working with SARs and/or respective variants according to its intended application (from sea/air interactions, biomass studies to topography and catastrophe control and prevention). The different nature of the application led to the creation of several different sensors employed on various platforms from commercial aircraft to spacecraft and even Uninhabited Aerial Vehicle (UAV)'s. Sensors actively on duty at the time of writing include but are not limited to:

- TanDEM-L (to be launched in 2023)
- BIOMASS (2021)
- NISAR (2021)
- RCM (2019 - present)
- SAOCOM (2018 - present)
- SENTINEL-1 (2014 - present)
- TanDEM-X (2010 - present)
- TerraSAR-X (2007 - present)
- Radarsat-2 (2007 - present)

The choice of available probes and sensors depends on the type of data the user intends to acquire, the required acquisition resolution (see fig. 2.6 for a sample TerraSAR-X image) and the final application of said data. Such applications may involve transportation, vegetation management, precision agriculture and disaster recovery.

Figure 2.6: Example of a TerraSAR-X High Resolution Image (Panama Channel).

2.10 Challenges

2.10.1 Optimum Frequency Band

Particular hindrances are still haunting SAR systems' performance up to this day, leaving room for improvement. One of its forms is, for example, attempting to find the optimum frequency band of operation which yields the maximum SNR value in the image for the targets of interest. If we take into account any particular atmosphere composition, RADAR height and range, there exists an optimum frequency band for SAR operation. Generally, as range increases and/or weather conditions become adverse, lower frequencies become more suited for the task at hand.

2.10.2 Signal to Clutter in Rain

While noise can obfuscate a SAR image, so too can competing echoes from undesired sources such as rain. Rain falling in the vicinity of a target scene will 'clutter' the image of that scene. Additionally, rain is not a static target, exhibiting its own motion spectrum. The motion spectrum typically is centered at some velocity with a recognizable velocity bandwidth. Taking these aspects in consideration, one can expect rain clutter effects to be noticeable only for the worst pluviosity rates, at the highest frequencies, at extremely coarse resolutions, and at considerable velocities. Nevertheless, while most airborne SAR's do not, some SARs do in fact operate under these conditions which warrants a thorough verification of rain clutter sensitivity. After all, a RADAR is meant to be an "all-weather" sensor.

2.10.3 Pulse Management

Next, we have also the issue of pulse management. Typical operation for terrestrial airborne SAR's is to transmit a pulse and receive the expected echoes before transmitting the subsequent pulse. This, of course, will place constraints on range versus velocity parameters for the SAR. One possible way to

circumvent this issue is to operate with pulses 'in the air', or in other words, transmitting new pulses before the expected arrival of a previous pulse's echo. This is entirely possible and is in fact routine in space-based SAR (where often a great number of pulses are transmitted prior to receiving an echo from the first pulse).

2.10.4 Range Extension

Last but not least, we are faced with the challenge of extending SAR range which is the equivalent to ensuring that an adequate SNR is achievable at the new range of interest. Methods to mitigate the range constraint include but not limited to:

1. increasing the average transmitter power
2. increasing the antenna area
3. modification of the operating geometry
4. employing coarser range resolutions
5. decreasing the velocity at which the antenna base is moving
6. decreasing system losses and/or the system noise factor

3

Imagery

Contents

3.1 Bands of Operation 25
3.2 Signal Polarization and Scattering 26
3.3 Speckle 28
3.4 Geometric Distortion 29
3.5 Imaging Modes 30
3.6 SAR Products 32
3.7 Rules of Thumb for SAR Image Interpretation 34
3.8 Available Tools 35
3.9 SOCET GXP® Tool Characterization 37
3.10 Context 38

Before we venture further into what can be done using SAR data and how to do it, it is best to introduce some relevant notions to keep in mind when dealing any kind of imagery and that is the relation between working wavelength and SAR bands.

3.1 Bands of Operation

Optical sensors collect data in the visible, near infrared, and short wave infrared portions of the electromagnetic spectrum. RADAR sensors on the other hand, such as the case of SAR, make use of longer wavelengths at the centimeter to meter scale, which confers it with unique properties such as the ability to see through clouds as mentioned. When it comes to dealing with SAR systems, the different operating wavelengths are often referred to as bands by letter designations such as X, C, L and P for instance. Table 3.1 shows a good summary of the operating bands as well as their association with frequency, wavelength and a typical, practical use of a particular band.

Table 3.1: SAR Bands of Operation.

Band	Frequency	Wavelength	Application
Ka	27 - 40 GHz	1.1 - 0.8 cm	Airport surveillance (rarely used for SAR)
K	18 - 27 GHz	1.7 - 1.1 cm	Water absorption (rarely used for SAR)
X	8 - 12 GHz	3.8 - 2.4 cm	High resolution SAR (urban monitoring, ice and snow, little penetration into vegetation)
C	4 - 8 GHz	7.5 - 3.8 cm	Main choice for SAR (global mapping, low to moderate penetration area monitoring, etc)
S	2 - 4 GHz	15 - 7.5 cm	Increasing use for SAR-based Earth observation and agriculture monitoring
L	1 - 2 GHz	30 - 15 cm	Medium resolution SAR (geophysical monitoring, biomass mapping, high penetration)
P	0.3 - 1 GHz	100 - 30 cm	Biomass, vegetation mapping and assessment, experimental SAR

Wavelength is an important feature to consider when working with SAR, as it determines how the RADAR signal interacts with the surface and how far a signal can penetrate into a medium. For instance, an X-band RADAR, which operates at a wavelength of about 3 cm, has very little capability to penetrate into broadleaf vegetation, and consequently, interacts with leaves at the top of the tree canopy most of the time. An L-band signal, on the other hand, has a wavelength of about 23 cm, achieving greater penetration into vegetation and allowing for more interaction between the RADAR signal and large branches or tree trunks (see fig. 3.1). Wavelength doesn't just impact the penetration depth into vegetation areas, but also into other land cover types such as soil and ice.

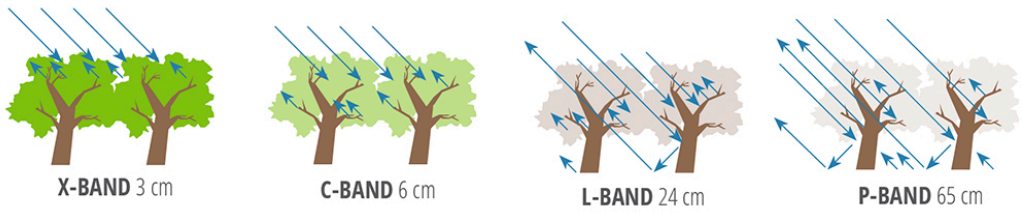

Figure 3.1: Sensitivity of SAR measurements to forest environment and depth of vegetation penetration at different wavelengths [6].

3.2 Signal Polarization and Scattering

RADAR sensors can also collect signals in different polarizations by controlling the analyzed polarization in both the transmitter and receiver paths. But what is polarization of a signal? It refers to the orientation of the plane in which the transmitted electromagnetic wave (the signal) oscillates. The horizontal polarization is indicated by the letter H, and the vertical polarization is indicated by V. The advantage of RADAR sensors is that signal polarization can be precisely controlled on both transmit and receive. Signals emitted in vertical (V) and received in horizontal (H) polarization would be indicated by a VH. Alternatively, a signal that was emitted in horizontal (H) and received in horizontal (H) would be indicated by HH, and so on. This feature is extremely important since it is possible to extract relevant information from the varying signal strength from these different polarizations such as the structure of the imaged surface, based on three scattering types: rough surface, volume, and double bounce or multipath. [15]

1. Rough surface scattering (or superficial scattering), such as that caused by bare soil or water, most sensitive to VV scattering.

2. Volume scattering caused by the leaves and branches in a forest canopy, most sensitive to cross-polarized signals like VH or HV.

3. Double bounce (or multipath) caused by buildings, tree trunks, or inundated vegetation, most sensitive to an HH polarized signal.

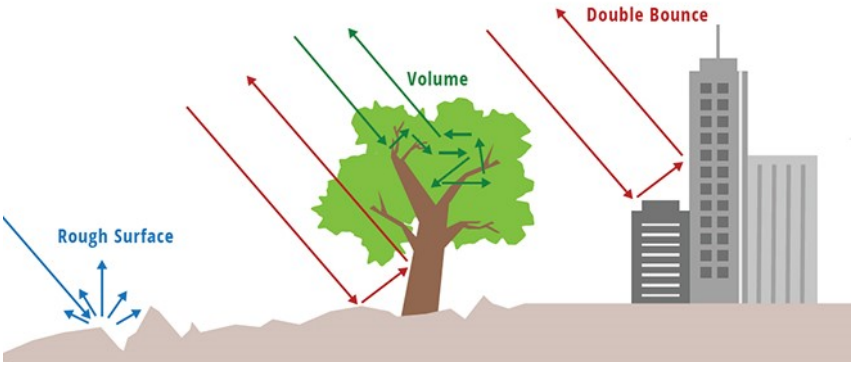

Figure 3.2: Scattering types in a real world scenario [6].

3.2.1 Superficial and Volume Scattering

The scattering behaviour of a given target is strongly influenced by the surface characteristics. If the surface is flat, the backscattering will be mainly specular, or in other words, akin to Fresnel's scattering.

This means that the electromagnetic wave will bounce in the opposite direction of the propagation direction. If the surface is rough, the backscattering will have a specific three dimensional pattern as seen on figure 3.2. Part of the transmitted energy will return to the sensor and this phenomenon is called rough surface scattering or “single bounce” scattering. On the other hand, if the target is made of elements whose dimension is comparable with the wavelength, much like the leaves of a tree for instance, the incident electromagnetic wave interacts with part of the volume of the leaves, or in other words, the signal travels deeper into the vegetation and in this case the scattering is called volume scattering. See figure 3.1 for a good illustration, this one depending on the operating band.

3.2.2 ”Double Bounce” or Multipath Scattering

If our target geometry is characterized by surfaces predominantly rectangular in overall shape and perpendicular between each other such as the case of buildings, a special phenomenon called multipath can be witnessed. In these circumstances, the RADAR signal, as it travels, suffers at least two or more bounces (reflections) before returning back to the sensor (see fig. 3.3). Examples of multipath scattering are not exclusive to situations where buildings are present. Other instances include bridges over flat water bodies, electrical lines, suspension beams on a bridge, other cylindrical objects of considerable dimension or even environments in which the relative position between several flat surfaces determine complex multipath effects such as the case of a city centre or a dense urban environment. [6]

It is important to mention that the amount of signal attributed to different scattering types may change as a function of wavelength since it changes the penetration depth of the signal. For instance, a C-band signal penetrates only into the top layers of the canopy of a forest, and therefore will experience mostly roughness scattering mixed with a limited amount of volume scattering. However a L-band or P-band signal will have much deeper penetration and therefore experience strongly enhanced volume scattering as well as increasing amounts of double-bounce scattering caused by the tree trunk. With that said, the correct selection of the SAR operating band is entirely dependent on the desired application.

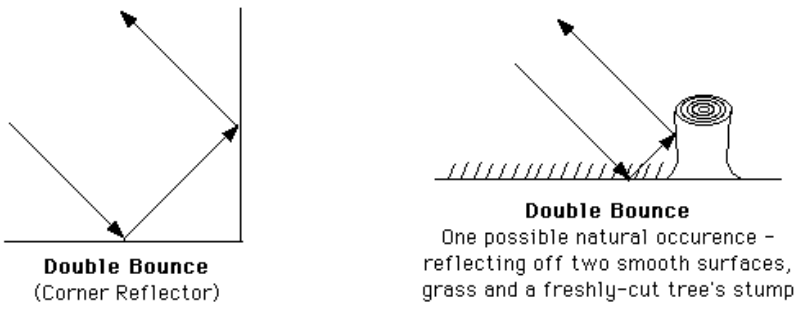

Figure 3.3: Double bounce scattering in different scenarios [7].

3.3 Speckle

All RADAR images appear with some degree of what we call RADAR speckle. Speckle appears as a grainy texture in an image. This is caused by random constructive and destructive interference from the multiple scattered returns that will occur within each resolution cell. An homogeneous target, such as a large grass-covered field, without the effects of speckle would generally result in light toned pixel values on an image. However, the reflections from the individual blades of grass within each resolution cell result in pixels sometimes brighter and sometimes darker than the average tone and so the field appears speckled.

Speckle is essentially a form of noise which degrades the quality of an image making its interpretation (visual or digital) more difficult. Thus, it is generally desirable to reduce speckle prior to interpretation and analysis. Speckle reduction can be achieved using multi-look processing which refers to the division of the RADAR beam into several narrower sub-beams. Each sub-beam provides an independent ”look” at the illuminated scene, as the name suggests. Each of these ”looks” will also be subject to speckle, but by summing and averaging them together to form the final output image, the amount of speckle will be reduced (see fig. 3.4).

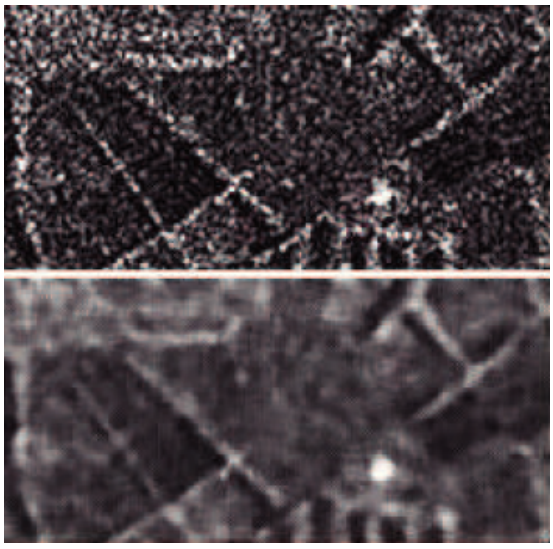

Figure 3.4: A before (top) and after (bottom) speckle reduction comparison of a RADAR image [8].

Multi-look processing reduces the speckle at the expense of resolution, since it essentially smooths the image. Therefore, the amount of the speckle reduction desired must be balanced with the particular application the image is being used for and the amount of detail required. If fine detail and high resolution is required, then little or no multi-looking/spatial filtering should be done. [16]

3.4 Geometric Distortion

There is another relevant aspect as far as data processing is concerned and that is geometric distortion caused mainly by mountains or similar structures. When a spaceborne SAR looks down and to the side toward a steep mountain, many objects on the mountain's facing slope may appear to be located at the same distance from the moving platform, as though the farther out in range an object is, the higher, or closer, to the spacecraft the ground is raised by the mountain to compensate. Since those many objects are located at nearly the same distance from the SAR, their backscattered signals will return to the spacecraft at about the same time. The SAR will conclude that the object located at that distance backscattered brightly, mapping all those returning signals into one location while in reality they came from many. This is called foreshortening, or layover (see fig. 3.5) in the extreme case where received signals from, for example, a mountain's peak are positioned before surrounding locations. [7]

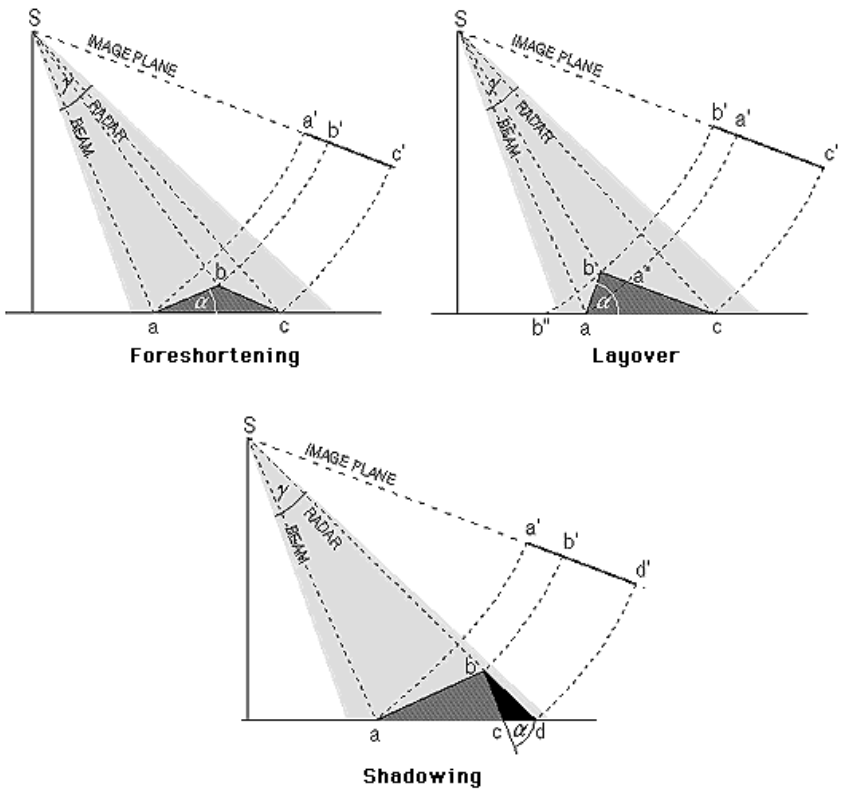

Figure 3.5: Geometric distortion types [7].

The resulting SAR image will show much of the mountain's bright facing slope was mapped onto a few pixels, while the darker backfacing slope was considered to cover many more pixels. Therefore it appears as though the mountains are lying over. Steeper topography or a smaller SAR look angle can worsen foreshortening effects.

As for geometric distortion caused by shadowing, it simply occurs when the area behind the mountain (or any given obstacle) cannot be detected by the sensor. Shadowing effects worsen with increasing look angles.

3.5 Imaging Modes

When it comes to acquiring imagery, different SAR sensors will feature different imaging mode variations. Despite of this fact, it is possible to state, on a more general perspective, three main imaging modes present in most sensors, each sensor with its specific variations: Stripmap mode, Spotlight mode and ScanSAR mode.

3.5.1 Stripmap Imaging Mode

In Stripmap mode is commonly known as the basic SAR imaging mode. The ground swath is illuminated with a continuous sequence of pulses while the antenna beam is fixed in elevation and azimuth. This results in an image strip with a continuous image quality in the direction of flight (see fig. 3.6). In order to achieve a consistent ground range resolution that matches the azimuth resolution, the transmitted pulse bandwidth is tuned specifically for each collection and is heavily dependent on the incidence angle.

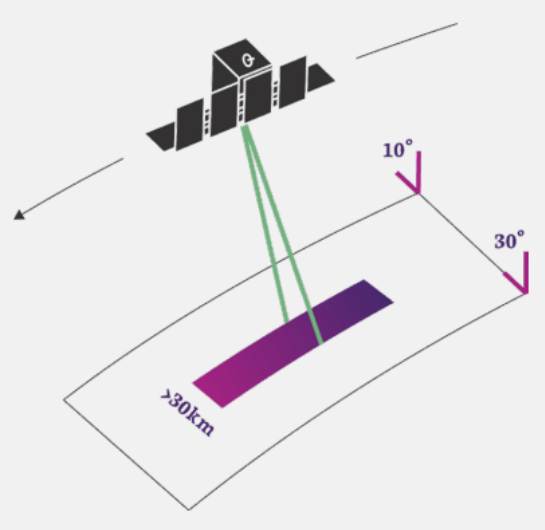

Figure 3.6: Illustration of the Stripmap SAR Imaging Mode [9].

Depending on the transmitted pulse bandwidth, the slant plane image resolution will vary accordingly. This product is then translated into a ground plane image with a specific resolution depending on the sensor settings and characteristics. For example, in some cases, a user may require a finer range resolution [9]. In these cases, some sensors offer the added imaging mode of Stripmap High Imaging

Mode. In this case, the product is available as a slant plane complex image that allows for precise target analysis. For convenience, the ground range product is often multi looked in range and azimuth to provide improved speckle reduction.

Some SAR systems, such as the case of TerraSAR-X, feature extended Stripmap Imaging modes involving twin or even quadruple polarization data. By recording the full scattering matrix using a dual receive antenna, allows the derivation of further polarization states such as circular or elliptic [17].

3.5.2 Spotlight Imaging Mode

In Spotlight mode, the RADAR beam is constantly steered towards an aim point on the ground (see fig. 3.7). This increases the time that the target area is illuminated, resulting in an increased synthetic aperture, and therefore, better azimuth resolution compared to a continuous stripmap mode.

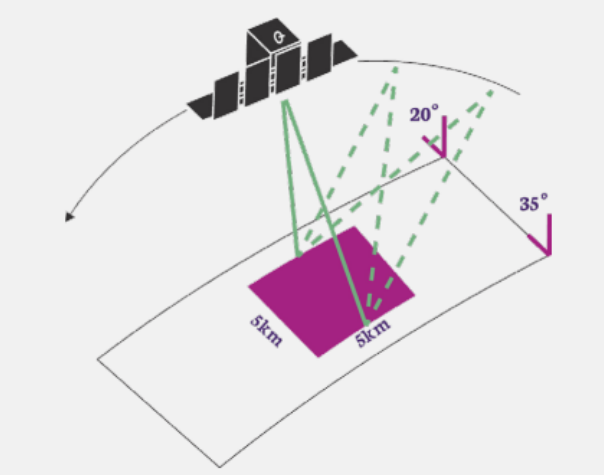

Figure 3.7: Illustration of the Spotlight SAR Imaging Mode [9].

As is the case of Stripmap mode, slant plane image resolution will also vary according to the transmitted pulse bandwidth and the this product is also then translated into a ground plane image.

3.5.3 ScanSAR Imaging Mode

In the ScanSAR imaging mode, electronic antenna elevation steering is used to acquire adjacent, slightly overlapping coverage areas with different incidence angles that are processed into one scene (see fig. 3.8). For systems such as TerraSAR-X for example, a swath width of 100 km or more is achieved by scanning four adjacent ground sub-swaths with quasi-simultaneous beams, each with different incidence angle. There are also other more advanced modes that allow for wider swath values which is the case of WideScanSAR [17].

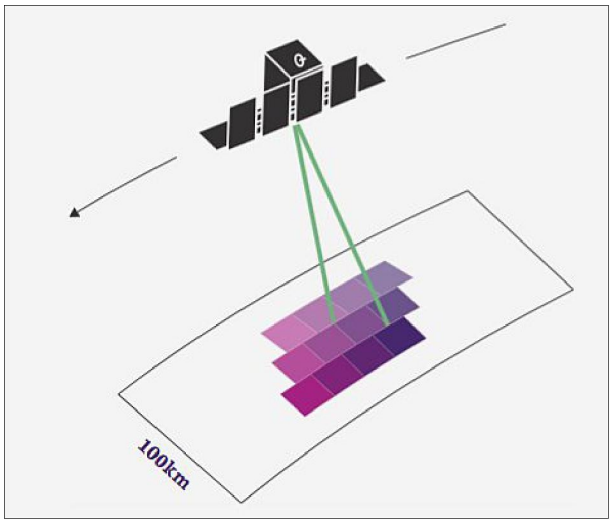

Figure 3.8: Illustration of the ScanSAR Imaging Mode [9].

3.6 SAR Products

It is important to keep in mind that a RADAR imaging system does not really know anything of imagery. The RADAR has no lens to focus light energy onto digital detectors from which image pixels are derived. As briefly mentioned in section 2.7, a SAR knows only about its raw measurements of time, magnitude, and phase, and they are manipulated with signal processing algorithms into images and other products. Refer back to fig. 2.5 for a helpful flowchart regarding the SAR product formation.

SAR imagery is often referred to as products having some sort of ranking such as L0 or L1 among other designations. A basic product is represented by a set of SAR image binary data along with the corresponding image annotation metadata, delivered as a singular product package. Products are characterized by the payload configuration (such as imaging mode and look direction) used by the respective satellite, as well as the level of processing that has been applied to the SAR scene. When it comes to the data geometric projection and representation, Level-1 image products are differentiated into two main product types: Single Look Complex (SLC) and Ground Range Detected (GRD).

3.6.1 Level-0 Products

Level-0 products usually contain the compressed and unprocessed Instrument Source Packets (ISP), with additional annotations and auxiliary information to support processing. These products require SAR processing and can be useful for SAR data processing testing purposes. Level-0 products are sub-divided into four product classes:

- SAR Level-0 standard products

- SAR Level-0 calibration products
- SAR Level-0 noise products
- SAR Level-0 annotation products

Standard Level-0 products represent the stream of ISPs containing SAR echo signal, calibration or noise signal. Level-0 calibration products represent the calibration pulses as extracted from the SAR ISPs stream. Level-0 noise products represent the noise and noise-equivalent (or travelling) pulses as extracted from the SAR ISPs stream. Level-0 annotations products contain the primary and secondary headers extracted from the SAR ISPs stream.

It is also important to note that Level-0 products may include data in single polarization mode (HH or VV) or, depending on the chosen imaging mode, they may include cross polarization modes (HH+HV or VV+VH). For cross polarization data, data for each polarization are available in separate files within the Level-0 product.

3.6.2 Level-1 Products

3.6.2.A Level-1 Single Look Complex (SLC) Products

Single Look Complex products are basic single look products of the focused SAR signal. Scenes are stored in the satellite's native image acquisition geometry which is the slant-range-by-azimuth imaging plane. The pixels are spaced equidistant in azimuth (according to the inverse of the pulse repetition frequency) and in slant range (according to the range sampling frequency). Each image pixel is represented by a complex magnitude value (with in-phase I and quadrature Q components) and therefore, contains both amplitude and phase information. Each image pixel is processed in the range direction, or in other words, perpendicular to the flight track.

The SLC products are suitable for applications that rely on phase information or require a finer degree of scene understanding provided by a finer resolution. There are no radiometric artefacts induced by spatial resampling or geocoding, and the product can be easily orthorectified using both commercial and free software tools such as European's Space Agency's Sentinel Application Platform (ESA SNAP S1TBX). The SLC product is particularly useful for those consumer groups that require interferometric collections or wish to exploit ground changes through Coherent Change Detection (CCD). The product is primarily intended for scientific research and development work, coherent analysis and for organisations with advanced SAR expertise.

3.6.2.B Level-1 Ground Range Detected (GRD) Products

Ground Range Detected products represent focused SAR data that has been detected, multi-look processed (averaged over range and/or azimuth resolution cells) and projected to the ground range using an Earth ellipsoid model. The image coordinates are oriented along the flight direction and along the ground range. The pixel spacing is equidistant in azimuth and in ground range. Ground range coordinates are taken from the slant range coordinates and then projected onto the ellipsoid of the Earth. For the slant to ground range projection, a specific ellipsoid and a scene-averaged value of terrain height is used and is annotated in the metadata. Pixel values represent detected magnitude. Phase information, unfortunately, is lost. The resulting product has approximately square spatial resolution and square pixel spacing with reduced speckle due to the multi-look processing. It is important to note that Spotlight Mode products are not multi-look processed.

3.6.3 Level-2 Geocoded Products

Geocoded (or geo-located) products consist of geo-located geophysical products derived from Level-1. Level-2 Ocean products, for example for wind, wave and currents applications may contain geophysical components derived from the SAR data such as Ocean Wind field, Ocean Swell spectra or even Surface Radial Velocity. This product is ideally suited for mapping applications and can easily be draped over a DEM, map or external image product using the encoded metadata. Pixel accuracy for this product will, therefore, be a function of the DEM used.

3.6.4 Level-3 and Level-4 Products

Level-3 products usually represent data or retrieved environmental variables which have been spatially and/or temporally re-sampled (derived from level 1 or 2 products). Such re-sampling may include averaging and compositing. Level-4 products model output or results from analyses of lower level data (variables that are not directly measured by the instruments, but are derived from these measurements).

3.7 Rules of Thumb for SAR Image Interpretation

At this stage, it is convenient to present some general rules when analysing SAR imagery before we move on to the next chapter where various examples and use cases are presented. These tips are meant to aid the reader in quickly spotting and extracting relevant information from any data in use.

1. Regions of calm water and other smooth surfaces will appear black, because the incident RADAR reflects away from the spacecraft.

2. Surface variations near the size of the RADAR's wavelength cause strong backscattering.

3. A rough surface backscatters more brightly when it is wet.

4. Wind-roughened water can backscatter brightly when the resulting waves are close in size to the incident RADAR's wavelength.

5. Hills and other large-scale surface variations tend to appear bright on the side that faces the sensor and dim on the side that faces away from the sensor. Mountains show this effect to the extreme, in part due to increased foreshortening.

6. Due to the reflectivity and angular structure of buildings, bridges, and other human-made objects, these targets tend to behave as corner reflectors and show up as bright spots in a SAR image.

7. A corner reflector can look like a bright cross in a processed SAR image since it is a particularly strong response.

3.8 Available Tools

Addressing the aforementioned limitations in the first chapter is a challenging process. Most of them are related to implementation parameters at the physical antenna level, local control and monitoring of performance parameters. Adjusting these parameters is out of the scope of this work and instead, the aim is to focus on the available tools and its capabilities at the data processing, visualization and analytical level. With this end in mind, a couple of software suites and toolboxes are available. Each and every one of them serves a particular purpose within SAR data processing requirements and does so in a more or less successful and efficient manner depending on the tool that is selected by the user and project requirements. Examples include but are not limited to:

3.8.1 PolSARpro (Biomass Edition) Toolbox

Developed since 2003 by the European Space Agency, the ESA PolSARpro Toolbox (Polarimetric SAR data Processing and Educational Toolbox) provides an Educational Software that offers a tool for self-education in the field of Polarimetric SAR data analysis and a comprehensive suite of functions for the scientific exploitation of fully and partially polarimetric data sets. The software proposes a great collection of well-known algorithms and tools and establishes a foundation for the exploitation of polarimetric techniques for scientific developments and stimulates research and applications developments using Pol-SAR, Pol-InSAR, Pol-TomoSAR and Pol-TimeSAR data. It also offers the possibility to handle and convert polarimetric data from a range of well established polarimetric spaceborne missions like ALOS-1

/ PALSAR-1, ALOS-2 / PALSAR-2, COSMO-SKYMED, GaoFen-3, RADARSAT-2, RISAT, TerraSAR-X, Tandem-X, SENTINEL-1A and B. [18]

3.8.2 ASF MapReady

The MapReady Remote Sensing Tool Kit allows users to process SAR data from a variety of missions, including datasets served by ASF and other providers, and some optical data. The tool allows user to terrain-correct, geocode, and apply polarimetric decompositions to multi-polarization SAR data. Despite all the available features, this toolkit is not suitable for processing Sentinel-1 products. The platform that MapReady supports is limited to older missions in ASF's catalog, including ALOS Palsar for instance. [19]

3.8.3 ENVI™ SARscape

ENVI™ SARscape by L3HARRIS™ can analyze SAR data and generate products like surface deformation maps, while giving the option to integrate this information with other geospatial products. This unique data analysis capability takes data from hard-to-interpret numbers, to meaningful, contextual information. Includes processing functionality for generating airborne and spaceborne SAR products based on intensity and coherence. This is complemented by a multi-purpose tool, which includes a wide range of functions – from image visualization to cartographic and geodetic transforms. [20]

3.8.4 BAE SYSTEMS SOCET GXP®

SOCET GXP® is a commercial geospatial intelligence tool used to identify and extract ground features for the creation of customized products from industry-standard imagery. The modern architecture provides ease-of-operation within a robust, reliable, and intuitive user interface providing maximum flexibility in information layout, manipulation and image processing. Capabilities support the ingest of imagery from both government and commercial sources to accurately display and export data in industry-standard formats.

It also provides a common framework to create, store, and share map data with the use of the Workspace Manager and the Multiport™. The Multiport® enables the viewing of the imagery and the functionality to extract features, create annotations, and develop 3-D simulations for product creation. It also allows users to make use of imagery in multiple formats. [21]

The first two mentioned tools, although freely available to the general public and with plentiful functionality, the case of PolSARpro for example, is heavily focused on Polarimetric SAR data processing. ASF MapReady capabilities are also constrained to past missions that are only in its catalog. That being said, the last two look a lot more promising, but are not free of charge, of course. After several contact

attempts, we were able to obtain a temporary student license for our dissertation purposes from BAE SYSTEMS resulting in SOCET GXP® being the tool of choice for this work and its main focus. With its ability to import and visualize imagery from a plethora of different sources and sensors as well as being able to perform relevant feature extraction, this is a powerful tool and a proper fit for the intended purpose of this work. It is worth mentioning that its vast complexity and functionality is not all relevant for this dissertation and so, we will be focusing only on its SAR capabilities.

3.9 SOCET GXP® Tool Characterization

While an enormous effort has been expended on systems to acquire SAR data, in comparison, little has been made with the intent of making the best use of said data. Software tools such as SOCET GXP® aim to solve this issue by bridging what we know about the data and the best way to get to and extract the relevant information they contain.

As was already shown in figures throughout this document, RADAR systems are capable of producing very high quality images of the Earth. But for this imagery to have any practical use or significant value, it must be interpreted in order to yield the information about the region which one might be studying. An active professional such as an image analyst can easily recognize features such as trees, fields, buildings, locations where water is present and other structures that encompass a wide range of both natural and man-made objects.

Despite the extent of the analyst's ability, it is a very time consuming task to extract the information and specially when large areas are concerned. Moreover, we are unable to guarantee consistency between studies if we don't know what tools to use, how they differ or how well they perform in a specific case or application. These limitations drive the exploration of these tools in an effort to derive relevant information more quickly and in a way that is reproducible. With that said, image analysis must encompass two main perspectives:

- A low level analysis that provides a series of methods to identify and quantify the details of an image's structure at the local level.

- A high level analysis that uses said details to build a global structural description of the site, which is what is required by an image analyst.

We hope that, at the end of this endeavour, anyone can get a good head start when it comes to dealing with SAR imagery, and more specifically, when the intention is to extract relevant features out of those data in a more timely manner.

3.10 Context

Understanding imagery is rooted mostly in experience and frequent exposure, both as regards to the broad human understanding of how the world is and in experimental findings that guide our perceptions of what particular aspects of an image should be examined more closely. As a basic example, most people not used to visualizing RADAR images would not immediately recognize the highlighted region in figure 3.9 as an urban area, but this sort of skill is quickly learned specially when using tools such as SOCET GXP®.

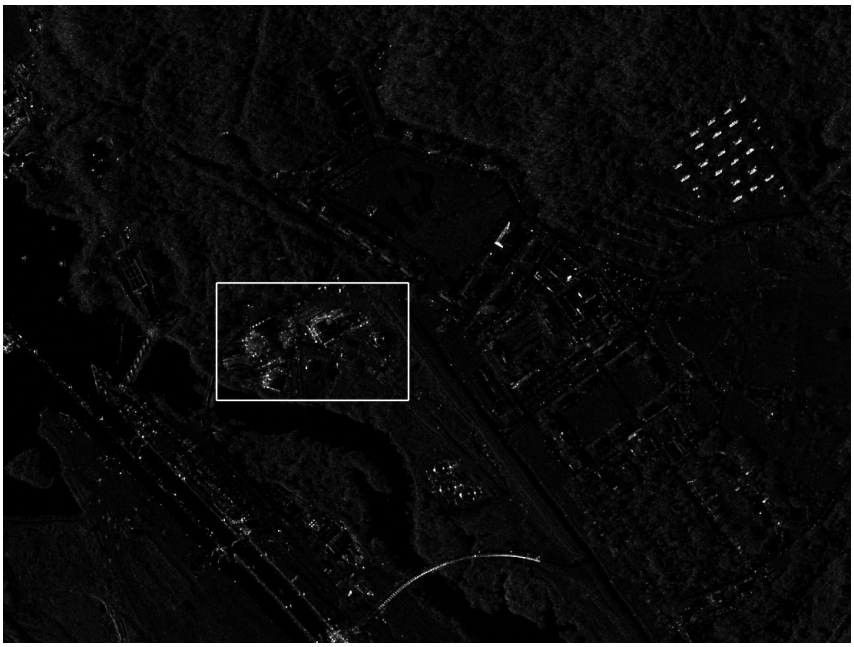

Figure 3.9: High-resolution image of the Panama Canal from sample data using SOCET GXP®.

It is precisely at this level that we intend to form a stronger basis of understanding such that more relevant information can be extracted faster in order that future work can be developed with such a tool. In a setting where the aim is to get a proper hands-on approach and when vast amounts of data are available from all kinds of different sources and probes, it is imperative to have a way of filtering through what is important and what is not. As beautifully put in [22], in a way, information can only be defined in the context of an application. Does an image tell the user something of interest to them? Let's also not forget the fact that the image is simply a representation of the local scattering properties of the Earth and all the information is carried by our knowledge of electromagnetic theory. Between the excessive particularity of the former and the over-generality of the latter lies a wide range of theory and technical development whose purpose is to provide a general approach to image analysis and understanding. Presenting this approach is the aim of this work.

4

SAR Tool Capabilities

Contents

4.1 Data Limitations 41
4.2 In-Software Approach 41
4.3 Histogram Features 43
4.4 Threshold LUT 44
4.5 Width and Height Measurements 44
4.6 Multi-Spectral Imagery Classification 45
4.7 Spectral Angle Mapper 46
4.8 Colorization 47

As mentioned before, when it comes to the format of the acquired data, for every piece of energy sent to the ground, two values are received: magnitude which is the amount of energy that gets reflected and phase which expresses the time that that energy took to return to the sensor. Next, these values come off the sensor as I and Q which represent complex numbers. SOCET GXP® then converts the Sensor Independent Complex Data (SICD) into magnitude and phase when the data is loaded. Finally, the data is divided into three main image components in a hierarchical fashion:

- Raw phase history data which comes directly from the sensor
- Complex imagery containing magnitude and phase information from sensor and is formed from raw phase data
- Detected imagery where only the magnitude is represented and formed from complex imagery. Has the disadvantage of missing valuable information such as time and depth.

4.1 Data Limitations

It is important to note that the amount of features and relevant information that can be extracted and inferred from a particular set of data is limited to the quality (or ”richness”, so to speak) of that specific dataset. The metric of quality should be expressed in terms of the user's intent. Some dataset characteristics (imaging mode, polarization, type of sensor, acquisition distance and duration, acquisition bands, etc...) might not be suitable for the user's intended purpose.

Throughout the course of this work, the selected data and results stem from the available datasets at the time of writing. Ideally, specific data should be requested for a particular location of interest. The process of requesting and obtaining such data is often not available to the general public and may not be accessible free of charge. For the purposes of this dissertation, the original idea was to obtain a proper data set from the Yucatán Peninsula in southeastern Mexico but since said data was not delivered in a timely manner, the presented work was performed using sample data from multiple sources such as L3HARRIS™, ICEYE, AIRBUS and MAXAR.

4.2 In-Software Approach

After gaining access to the desired imagery, the first point to address should be Anamorphic Correction. Since raw sensor data is often not square, it is recommended to square the image pixels by anamorphically correcting them within the tool. This way it is possible to obtain more pixels in the range or crossrange directions and presents a cleaner picture. It is important to note that despite this fact, square pixels may lose some spatial resolution during the correction process.

Next, and before commencing any analysis, it is convenient to consider the slant to ground plane where it id possible to switch the visualization of the active Multiport™ panel between slant visualization and ground plane visualization for complex SAR data (see fig. 4.1). This functionality stretches the image pixels while still maintaining the original rigorous sensor model.

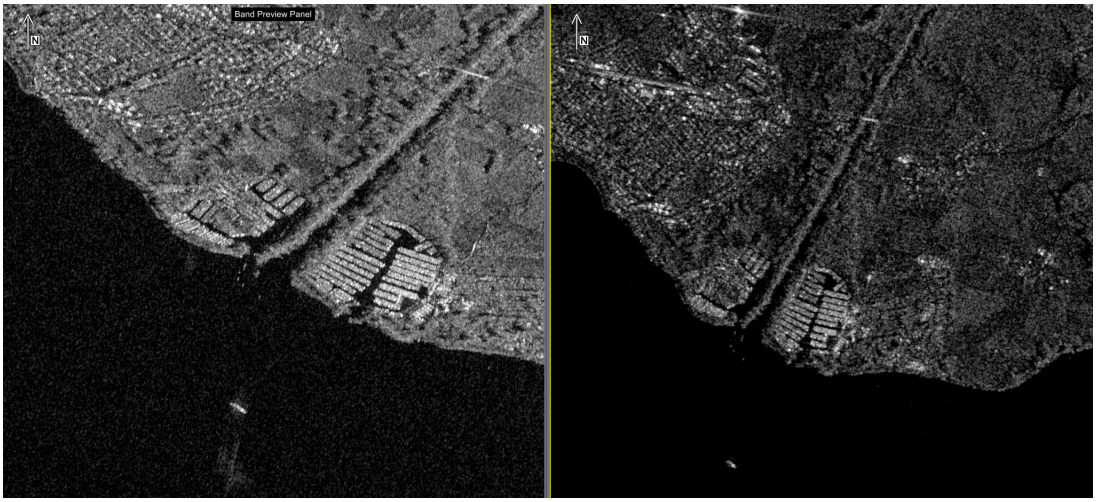

Figure 4.1: Slant (left) and ground (right) plane visualization rendered from sample data using SOCET GXP® (Lake Constance, Germany).

Finally, we can also enable the SAR Overlay (see fig. 4.2) to graphically display SAR metadata that is either extracted or computed from image tags. It provides an indication of the degrees for Flight, Shadow and Layover.

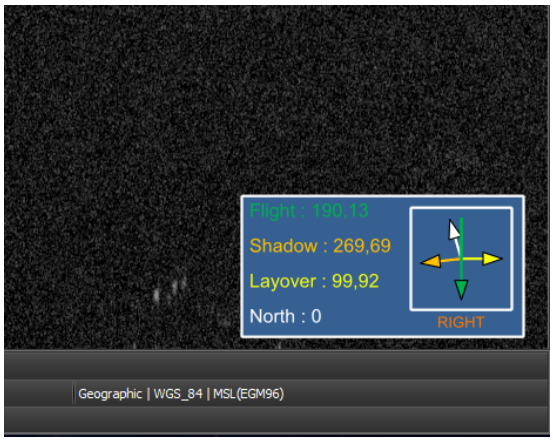

Figure 4.2: SAR Overlay enabled using SOCET GXP®.

4.3 Histogram Features

By taking advantage of the distribution of the image pixel values, we're able to use the histogram features built-in. The histogram tool dismisses pixel values equal or close to zero and "stretches" the remaining values to then obtain a brighter, sharper image. The thresholds at which this cut-off is performed can be adjusted in the Lower and Upper percentage cut-off inputs. This panel shows the number of times a particular pixel value occurs in the image where the horizontal axis indicates the pixel value and the vertical axis denotes the number of pixels at that particular value.

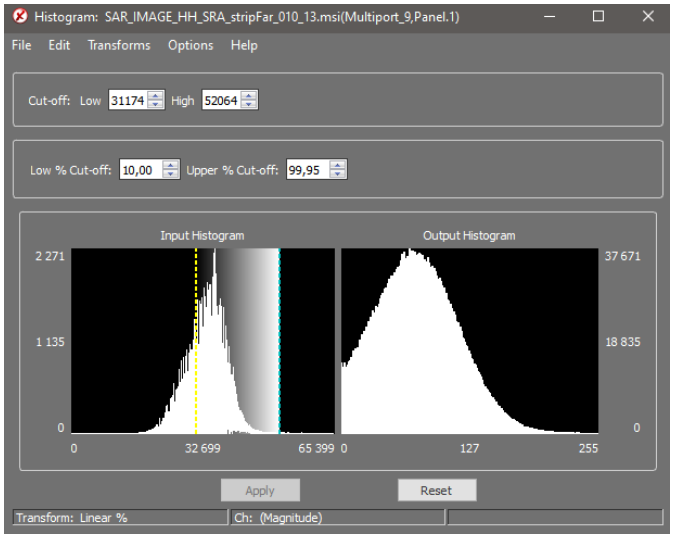

Figure 4.3: Image histogram using SOCET GXP®.

The input histogram on the left in fig. 4.3 displays the histogram for the raw data where a low digital number is shown as a black color in the image and a high digital number appears white. Upon opening an image file, it is automatically remapped and the results of this remapping are shown in the output histogram on the right. Of course, the result of the histogram changes whenever the user "looks" to a different region within the image.

Moreover, the image histogram can be manipulated using transforms through a standard set of algorithms. The available transforms include:

- **Linear 2%** - Applies a linear transform with a 2% clip on both ends of the histogram
- **Linear Min/Max** - Data range linearly re-maps to fill the dynamic range of the display by applying a linear transform with the clip values set to the data minimum and maximum on either end of the histogram
- **Normalization** - Re-maps data to fit a bell-shaped curve which is useful for visual comparison of images

- **Equalization** - Reduces contrast in very dark or very bright areas and increases contrast in mid-range areas
- **Square Root** - Reduces the gray level range of images with histogram skewed towards lower gray levels

This specific feature is one of the ways of determining certain terrain characteristics such as water resources, for example, by exploiting the distinct pixel signature inherent to the RADAR signal response of water. This and other scenarios will be explored in chapter 5.

4.4 Threshold LUT

Look Up Tables (LUT) allow users to map pixels of certain values or ranges to other various colors. The Threshold LUT functionality modifies the pixels of an image according to a defined percentage. For example, we may choose to display a specific band by itself and display a percentage of the brightest pixels present in that particular band:

Figure 4.4: Threshold values at: 0 (left), 50 (center), 99 (right) using SOCET GXP® (Lake Constance, Germany).

For instance, when we set the threshold value to 99 (see fig. 4.4), only the top 1% of pixels remain on display which can be useful for detecting hotspots (as in the highest pixel values). If we are presented with a landscape and we aim to find out where in that landscape a specific element (like clay, for example) is more heavily present, we know that in that particular band is where clay is going to spike and is often the only present signature after applying this LUT threshold.

4.5 Width and Height Measurements

It is also possible to quickly measure features and objects on imagery (see fig. 4.5 and fig. 4.6). Let us suppose that we wish to measure the width of a plot of land. We can make use of the acquired data and the tool to determine its width accurately. The height of a building can also be determined.

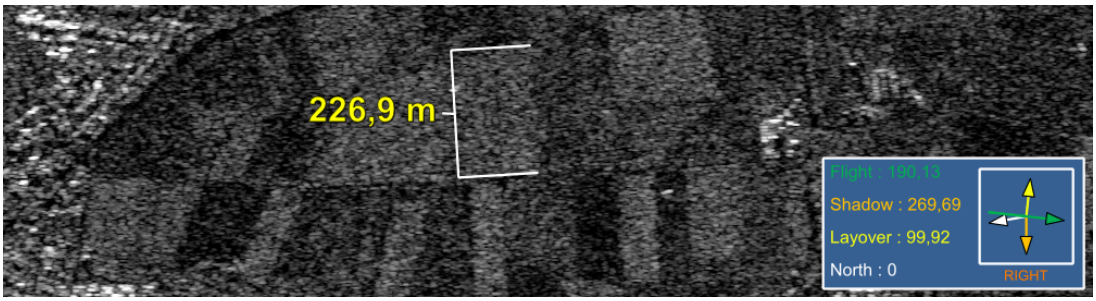

Figure 4.5: Farmland plot width measurement using SOCET GXP® (Lake Constance, Germany).

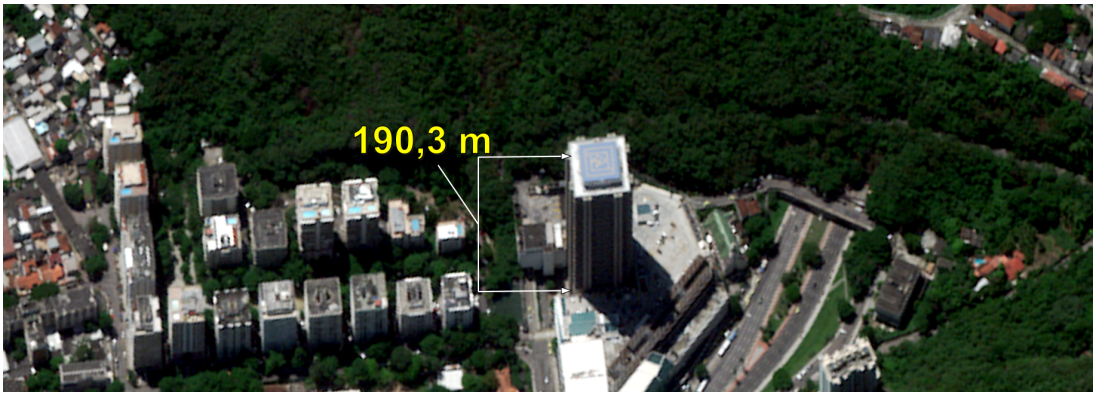

Figure 4.6: Building height measurement using SOCET GXP® (Rio de Janeiro, Brazil).

4.6 Multi-Spectral Imagery Classification

Traditional 4-band Multi-Spectral Imagery (MSI) contains bands of red, green, blue and near-infrared. Each band can be assigned to any of the R, G, or B channels displayed on the Multiport®. Upon obtaining compatible data, true-color imagery is what the human eye sees which results from assigning the red, green and blue bands to their respective red, green and blue channels. With MSI imagery we can assign bands to different RGB values in order to highlight items or regions of interest such as healthy or dying vegetation, for example. And the more bands we have available within the dataset, the more combinations can be displayed. Let us take a look at an example of Rio de Janeiro's coastal area in Brazil.

As is evident in fig. 4.7, we can observe the effects of spectral selection on areas with certain types of vegetation and/or in certain conditions. The different red color gradients serve as an indicator of whether or not vegetation in a particular area is well watered/healthy or not. Proper quantification can also be performed by taking a look at the exact magnitude values shown by these particularly highlighted areas.

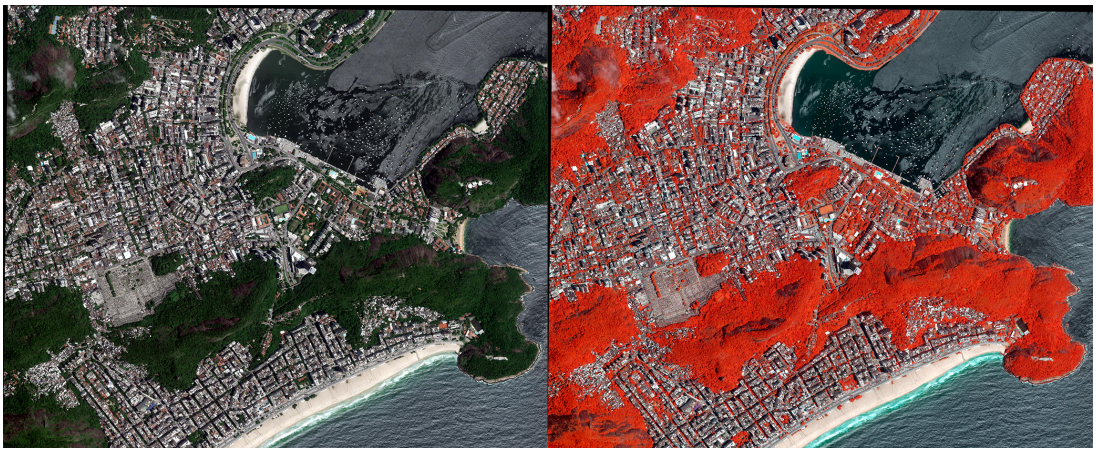

Figure 4.7: Band filtering with near-infrared selection at 833 nm wavelength using SOCET GXP® (Rio de Janeiro, Brazil).

4.7 Spectral Angle Mapper

The Spectral Angle Mapper functionality falls within the Supervised Classification category where algorithms are used to match in-scene pixels to an existing spectral signature. The classification is supervised in the sense that it is the user who selects the pixels to find in the scene and the algorithms to identify similar pixels which account for each band in the image. In this type of classification, the angle between vectors created by two spectral signatures is measured. Figure 4.8 shows an example of the output product using Spectral Angle Mapping supervised classification of vegetation (in green), roads (in red) and water (in blue).

Figure 4.8: Supervised classification of vegetation, roads and water using SOCET GXP® (Tripoli, Libia).

This feature presents itself as yet another way of estimating vegetation area. Moreover, we can also make use of spectral libraries where a list of materials with known spectral signatures is present. With

this information, one can, for example, find in the scene evidence for the presence of certain types of vegetation such as Willow Sedge, Whitebark Pine, Lodgepole Pine among other species of commonly found vegetation.

4.8 Colorization

Detecting the presence of water on any given surface is an essential application. It prevents the actual, physical inspection of the site in question and further debate as to whether or not to select that particular location for farmland or reject it as an unreliable construction site. By taking advantage of the colorization features of SOCET GXP® we are able to tell with reasonable accuracy the location of water resources such as rivers, creeks and ponds.

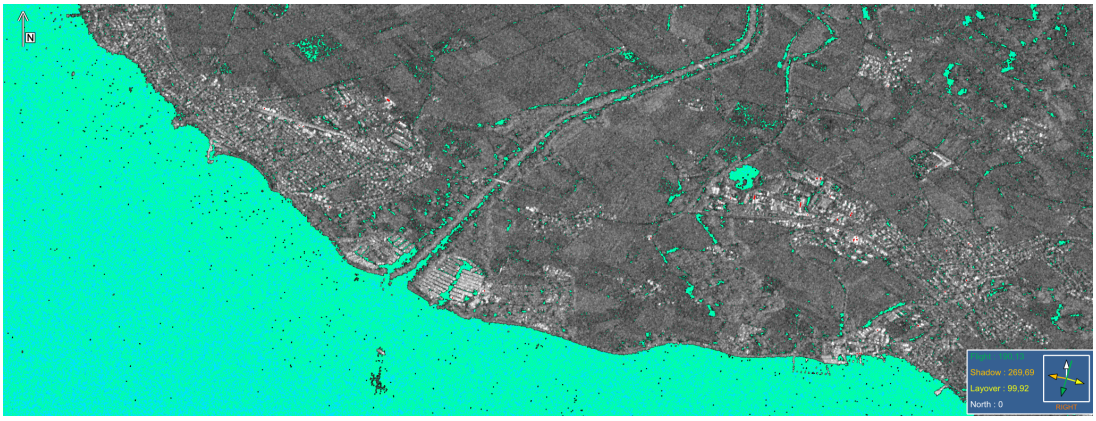

Figure 4.9: Water resource detection through colorization using SOCET GXP® (Lake Constance, Germany).

The results shown in fig. 4.9 were obtained by locking in the spectral signature of the large body of water surrounding the region and then assigning a particular color (in this case, a cyan green gradient) to areas where the complex signal values are similar. It is also important to note that the figure shows a juxtaposition of two sets of imagery from the same site, the first acquired in HH polarization and the second in VV polarization.

The full range of capabilities of SOCET GXP® goes beyond the scope of this work. To cover them in their entirety would easily require a dedicated dissertation, and an extensive one at that. Since the aim of this work is to explore what can be done pertaining to SAR images, the aforementioned capabilities are more than enough to be applied in a useful way to real-world challenges. We will address them in the following chapter.

5

Use Cases

Contents

5.1 Foreword 51
5.2 Soil Moisture Estimation 51
5.3 Subsidence Estimation 52
5.4 Forest Height Estimation 53
5.5 Oil Spill Detection 55

From the previous chapter, one can conclude that just some of the SAR capabilities can translate into several real world scenarios where such capabilities might be of great use. In the following sections, some examples as to how one can make use of such tools is shown for multiple circumstances.

5.1 Foreword

Unfortunately, and due to what was already mentioned in section 4.1, the intended structure and contents of this chapter underwent modifications in comparison with what was originally intended. Challenges such as water resource detection and vegetation health assessment were meant to be covered using SOCET GXP® but due to the lack of ”rich” data availability, continuing to analyse and process sample data (as was the case in the previous chapter) would become redundant since there’s only so much information (and useful information at that) one can extract from said data. The end result would be feature extraction that would not translate in necessarily concrete information about a specific problem.

For example, for the case of vegetation health assessment, it would be useful to obtain an estimate of the total forest area that would meet a specific health threshold based on its spectral signature but then again, without specific data, it cannot be determined in an accurate manner. We would need data acquired in the S and P bands for instance (see table 3.1) and requesting and obtaining it, depending on the provider, can cost from hundreds to thousands of dollars per unit area. Despite attempting to come in contact with several SAR data providers requesting said data for the purposes of this dissertation, we obtained no response whatsoever and were forced to make a decision.

That being said, in this chapter we will still address real world scenarios but since we are unable to use the intended tool with the desired data, we will instead make use of the sparsely existing literature to exemplify some of the intended use cases, and more specifically, use as reference publications that can be found in [10] and [11].

5.2 Soil Moisture Estimation

Scattering mechanisms can be exploited to derive qualitative and quantitative physical information for land, snow and ice, ocean and urban applications. In other words, by taking advantage of SAR polarimetry and based on the measurement and exploration of the polarimetric properties of man-made and natural scatterers. Shape, orientation and dielectric properties of the scatterers can be obtained and allows the development of physical models for the identification and/or separation of scattering mechanisms occurring inside the same resolution cell.

Polarimetric decomposition techniques have been successfully used to separate and remove undesired vegetation signal contribution and allow estimation of the soil moisture content.

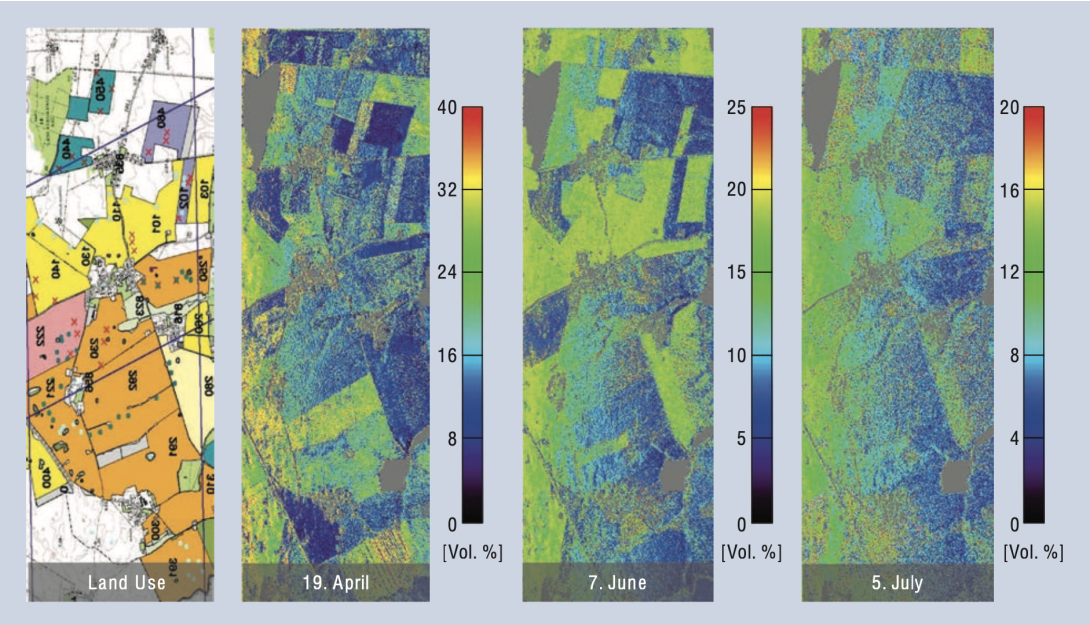

Figure 5.1: Soil moisture maps obtained after applying polarimetric decomposition to remove the vegetation layer and inverting the remaining ground component [10].

In fig. 5.1, we can visualize the soil moisture maps obtained from polarimetric L-band SAR data acquired at three different dates. At the time of the first acquisition in April, the crop layer was still short and light. Its height and density increased during the next acquisitions performed in June and July. If we were to use SOCET GXP® as originally planned, we would be able to produce similar results involving moisture gradients which would then translate into practical values pertaining to soil moisture volume in percentage as depicted.

5.3 Subsidence Estimation

Before addressing this use case, it is convenient to briefly mention SAR interferometry (InSAR) and differential interferometry which were the techniques used to obtain these results. SAR interferometry refers to yet another powerful remote sensing technique that enables the highly accurate measurement of important geophysical parameters such as surface topography, ground deformation and subsidence as well as glacier movements. In short, the goal for a given scene is to compare the phase of two or more complex RADAR images that have been acquired from slightly different positions or at different times. Since the phase of each SAR image pixel contains range information that is accurate to a small fraction of the RADAR wavelength, it is possible to detect and measure small path length differences with accuracy in the centimeter to millimeter range.

As for SAR differential interferometry (DInSAR), similar as with InSAR, the high sensitivity of a SAR

instrument to measure the LOS propagation distance is exploited in order to detect displacements of the Earth surface at a wavelength scale. Two SAR images are also acquired with a certain temporal separation that are combined to generate an interferogram. Next, and by using an external DEM, the topographic information can be subtracted from the interferogram, leading to a differential SAR interferometric measurement where subtle changes of the range distance between the two acquisitions (e.g., due to subsidence) can be detected.

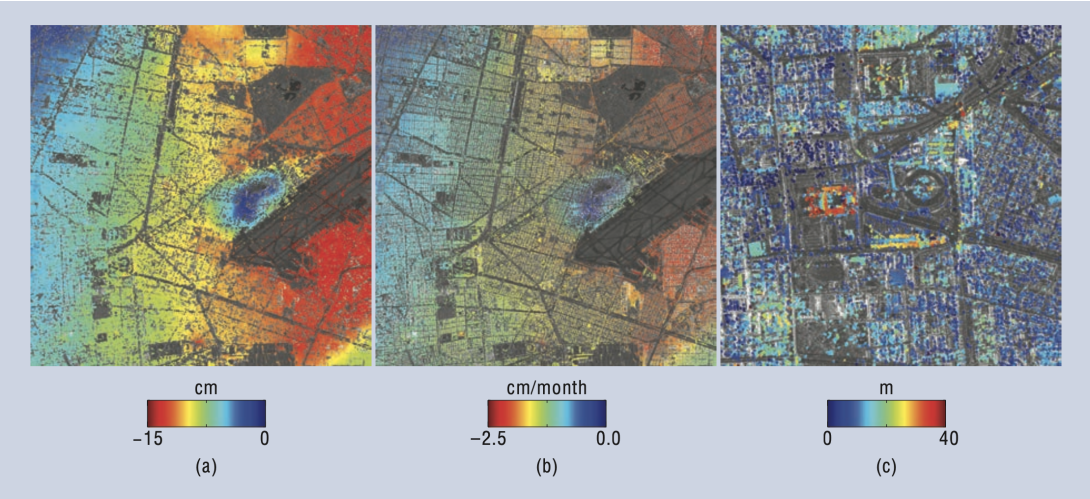

Figure 5.2: (a) Estimated subsidence over Mexico City obtained with two TerraSAR-X images acquired with a 6 month difference (overlay of reflectivity and phase) (b) Mean deformation velocity estimated over Mexico City (c) Zoom over the city of the refined DEM retrieved as an additional product to the deformation velocity, where the individual buildings can be observed. The scene size is approximately 8 km x 8 km. RADAR illumination from the right [10].

Figure 5.2 shows the subsidence over Mexico City estimated with two TerraSAR-X images acquired with a 6 month difference. We can observe that the maximum displacement is about 15 cm in some city areas. The subsidence is due to ground water extraction and it is a well-known problem in Mexico City. Provided that we could have access to such data, similar results could also be obtained using SOCET GXP®. By taking advantage of the temporally spaced RADAR acquisitions in addition to the topographic information as well as reflectivity and phase information it would be possible to simulate a similar subsidence map, albeit with different color gradients.

5.4 Forest Height Estimation

This next use case involves the use of Polarimetric InSAR (Pol-InSAR). Pol-InSAR is today an established technique that promises a breakthrough in solving essential RADAR remote sensing problems. Across the different application fields forest parameter retrieval is by far the most developed one and for the purposes of this work we will be addressing forest height which is important for ecological pro-

cess modeling and monitoring and the understanding of ecosystem change. A single baseline quad-polarization acquisition is sufficient for the estimation of forest height.

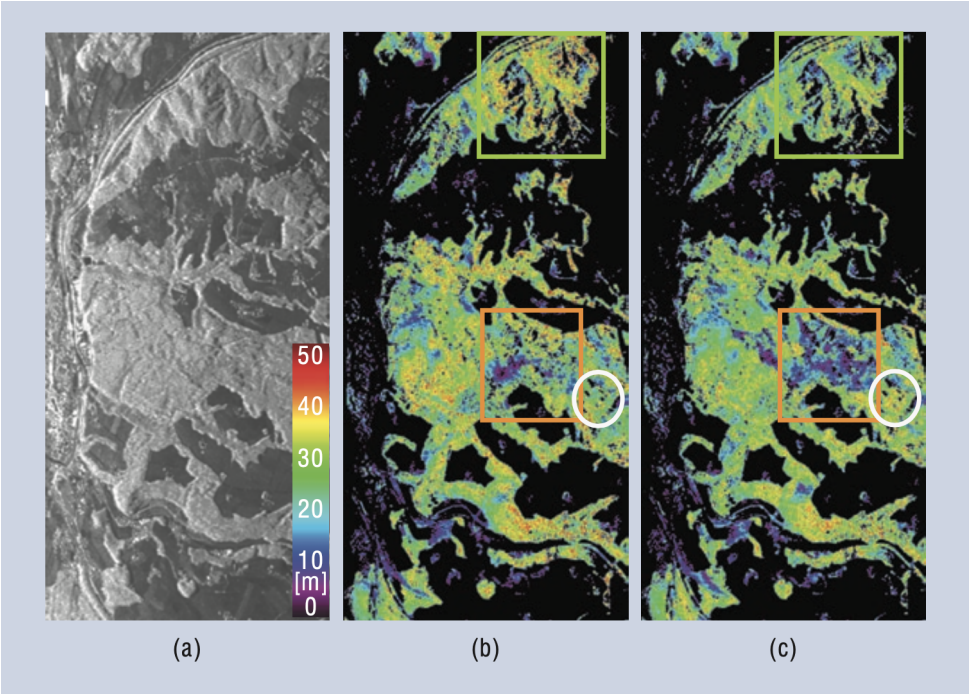

Figure 5.3: (a) L-band HV intensity image of the Traunstein test site. Forest height map computed from Pol-InSAR data in (b) 2003 and (c) 2008 [10].

In fig. 5.3, an L-band SAR image of the Traunstein forest site, located in southern Germany is shown. The Traunstein forest is characterized by a large variety of forest stand conditions in the presence of locally variable topography. In the middle and on the right of the figure we can visualize forest height maps derived from Pol-InSAR data acquired at L-band in 2003 (b) and 2008 (c).

Comparing the two forest height maps a number of changes within the forest become visible: The logging of individual tall trees as a result of a change in forest management between 2003 and 2008 (marked by the green box); the damage caused in January 2007 by the hurricane Kyrill which blew down large parts of the forest (marked by the orange box); and finally forest growth on the order of 3 to 5 m over young stands as seen within the area marked by the white circle. In the context of this dissertation, the selected tool could be used to obtain similar maps either taking advantage of the Colorization features (see section 4.8), Multi-Spectral features (see section 4.6) or even Spectral Angle Mapping (see section 4.7) for more accurate results.

5.5 Oil Spill Detection

SAR images can also be extremely useful when detecting oil spills. These spills can originate from discharges from ships or even offshore extraction platforms. Oil pollution from sea-based sources can be accidental or deliberate. Fortunately, the number of marine accidents and the volume of oil released accidentally are in decline. On the other hand, routine tanker operations can still lead to the release of oily water and tank washing residues. Furthermore, fuel oil sludge, engine room wastes and foul bilge water produced by all kinds of ships, also end up in the ocean. In the last decade, maritime transportation has been growing steadily and so, more ships increase the potential number of illegal oil discharges. Whatever the case may be, oil is a major threat to the sea ecosystems and SAR is of very great use in mitigating this issue. The possibility of detecting an oil spill in a SAR image relies on the fact that the oil film decreases the backscattering of the sea surface resulting in a dark formation that contrasts with the brightness of the surrounding spill-free water.

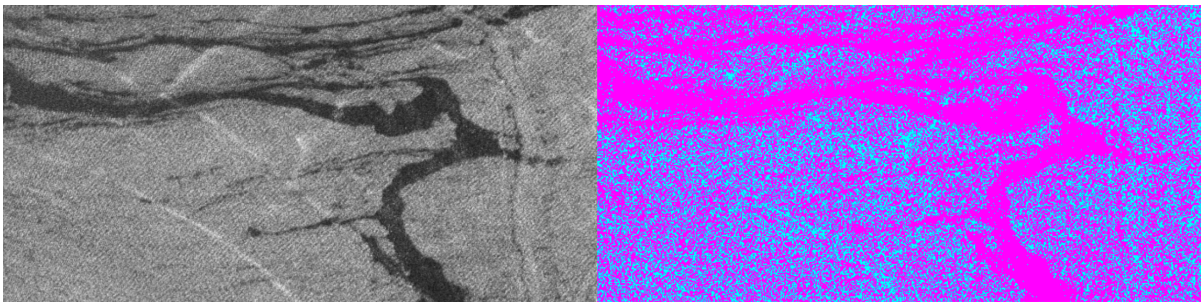

Figure 5.4: Original oil spill SAR image (left) and post-classification SAR image (right) [11].

In fig. 5.4 we can observe the 2010 Dalian Xingang oil spill event in Japan. From the original SAR image, the darker areas correspond to the oil contents in the ocean. This particular example was selected since it wielded the most resemblance to the results that would be obtained in SOCET GXP® with the adequate data and using Colorization (see section 4.8) in conjunction with Spectral Angle Mapping (see section 4.7) or even Threshold LUTs (see section 4.4). The paper does not mention from which sensor the data originated neither its acquisition mode or polarization.

Whatever the case may be, data of the location acquired in the C-band would be adequate due to the fact that, in this frequency range, low wind speeds create sufficient brightness in the image and make the oil film visible. Despite the fact that oil spill identification is largely dynamic depending on how recently the spill occurred, image resolution and RADAR illumination incidence angle, from this specific dataset it would be possible to obtain a fairly accurate estimate of the oil spill area. Moreover, in conjunction with known information about the physical properties of oil and its behaviour dynamic when amidst sea water, it would also be possible to obtain a fair estimate of the total volume of the spillage.

6

Conclusion

Contents

6.1 Overview 59

6.2 Future Work 60

6.3 Final Remarks 61

6.1 Overview

In the last decades we have witnessed a tremendous increase of Earth observation applications that take advantage of the unique properties of SAR images in various resolutions, polarization combinations and acquisition modes. To study dynamic processes on the Earth surface, more and more users ask for ever increasingly complex and rich RADAR imagery. Consequently, these same users also search for various visualization and processing tools that are able to push their work as analysts to the next level in order to achieve the ultimate goal of delivering better, more actionable results in an efficient and timely manner. And as the quantity of data increases rapidly, it also amplifies the need of such a tool.

With this in mind, throughout the course of this work we sought to achieve two main goals:

1. Find a SAR imagery analysis tool that could deliver prompt and useful results from virtually any relevant imagery source

2. Provide a hands-on approach to SAR imagery analysis with the aid of the aforementioned tool.

Upon exploring and evaluating some of the existing tools (in section 3.8), SOCET GXP® fulfilled the intended purpose with distinction, specially considering the data that was available at the time of writing and its limitations (refer to section 4.1). This document is primarily targeted to readers new to the use of SAR imagery and who want to gain relevant insight on what first steps to take in order to begin exploring the possibilities of SAR while producing relevant outputs without having to spend huge amounts of time looking into the technicalities of RADAR imaging before being able to deliver useful results. Taking this in consideration, by this point in the document it is fair to state that the target reader is now fully aware of the essential principles pertaining to RADAR from a scientific standpoint, how these principles relate to SAR imaging and also how they translate into key concepts when dealing with imagery.

The reader is now able to know what data particularities to look out for considering the intended application of the work to be performed as well as how to take advantage of said particularities using SOCET GXP® to achieve the desired goal when it comes to feature extraction for that application. It also important to mention that a full, extensive coverage of all of the tool's functionalities would easily warrant a separate dissertation and, at the same time, would defeat the purpose of this work in the sense that it would not be able to provide such an actionable guide "out of the box" when it comes to SAR imagery, but instead, an extensive manual-like document. It would require of the reader the knowledge of additional information present (hopefully) elsewhere.

This document bridges exactly that gap. Not withstanding, this dissertation would greatly benefit of the availability of proper data not only for illustration and guidance purposes but mainly for the production of useful results in the context of the selected tool when it comes to real world scenarios and applications being this aspect its main fault.

6.2 Future Work

Furthering this work will undoubtedly be dependent on the richness of data, how adequate and available said data is in relation to its intended application and also on further advances when it comes to SAR imaging technology and processing. Surprisingly enough, SAR sensors and more specifically spaceborne SAR sensors have been around for more than 40 years. The first official SAR launch took place in 1978, it was NASA's Seasat satellite, a spaceborne platform with the purpose of monitoring oceanographic phenomena. It carried an L-band SAR with HH polarization that was mounted at a fixed angle to observe global surface wave fields and polar sea ice conditions. Despite its short lifetime, this sensor paved the way to what SAR sensors would become today and beyond, demonstrating the capability of such technology for both ocean and land surface observation. From here on out, the possibilities were only limited by imagination and multiple possible applications and developments ensued.

The current generation of SAR instruments is, however, limited in their capability to acquire RADAR images with both high-resolution and wide-swath coverage. This immediately impacts the acquisition frequency if large contiguous areas shall be mapped systematically with a single satellite. The resolution versus swath width restriction is fundamental and closely connected to the intricacies of the SAR data acquisition process. Taking that and other factors into context, the future SAR development landscape will likely be impacted by:

1. Increased **data availability** specially when it comes to ease of access and "richness"
2. Further developments when it comes to **advanced imaging techniques**

6.2.1 Data Availability

Despite the fact that some previously restricted SAR datasets are becoming more available (such as the sample imagery datasets used in this document), these do not carry the full spectrum of possibilities from a user standpoint that is not part of the commercial sphere as is the case here. A shroud of secrecy is still present and, although justifiable or understandable in part, it hinders further advances on behalf of the general public. On the bright side, there are upcoming missions promising multi-band data and advocating free and open data policies. These will greatly benefit the public archive of RADAR imagery of the Earth.

Of course, this opportunity also poses future practical challenges to image analysts as well as geospatial departments, specifically when it comes to processing and storing large volumes of SAR data and derived products. It is anticipated that publicly accessible platforms where state-of-the-art data can be downloaded (or at least viewed) will gather more and more significance as users begin finding out the importance of SAR imagery and respective applications. And specifically, platforms that do not

bar users behind pay walls or commercial/government clearances. The forthcoming NISAR mission is predicted to generate more data than any NASA Earth observation mission (up to 85 TB of data each day) and a project is already underway in an effort to prepare users for the migration to the commercial cloud [23]. On the other hand, while this may mean the free availability of data, it also raises concerns on the free manipulation of said data and its respective possession or ownership. Nonetheless, debating the ethics of such measures is out of the scope of this work.

6.2.2 Advanced Imaging Techniques

Several SAR imaging modes have been developed that provide different trade-offs between spatial coverage and azimuth resolution. Examples are the ScanSAR mode (see section 3.5.3), which enables a wide swath at the cost of an impaired azimuth resolution, and the Spotlight mode (see section 3.5.2), which allows for an improved azimuth resolution at the cost of a non contiguous imaging along the satellite track. However, it is not possible to combine both imaging modes and to overcome this issue, several innovative digital beamforming techniques have been presented where the receiving antenna is split into multiple sub-apertures that are connected to individual receiver channels.

The digitally recorded signals are combined to simultaneously form multiple independent beams and to gather additional information about the direction of the scattered RADAR echoes. This information can be used to increase the receiving gain without a reduction of the imaged area by switching between narrow, high gain beams, as well as gain additional information about the dynamic behavior of the scatterers and their surroundings. A good example is the currently under development high-resolution wide-swath (HRWS) SAR at EADS Astrium [24]. The system has been specified to map a 70 km wide swath with a resolution of 1 m, thereby exceeding the number of acquired ground resolution cells of the TerraSAR-X Stripmap mode (3 m resolution at 30 km swath width) by a factor of 21.

6.3 Final Remarks

In an ever changing and dynamic world, geospatial information with global access and coverage becomes more and more important. Constellations of spaceborne satellites as well as airborne sensors play a major role in this task considering that SAR is the only all weather, day and night sensor. With the various applications already mentioned, the future for SAR remote sensing looks promising. Tools like the one used in this work alongside wide data availability originating from sensors equipped with highly innovative concepts hereby mentioned will allow the global observation of dynamic processes on the Earth's surface with unparalleled quality and resolution. It will open the door to a future global remote sensing system with high resolution imagery and relevant geospatial information updated by the minute.

Bibliography

[1] Sandia National Laboratories, “Pathfinder Radar (ISR) and Synthetic Aperture Radar (SAR) Systems,” Website. [Online]. Available: https://www.sandia.gov/radar/what_is_sar/index.html

[2] NASA Jet Propulsion Laboratory, “Color Image of Death Valley, California from SIR-C,” Website, 1999. [Online]. Available: https://photojournal.jpl.nasa.gov/catalog/PIA01349

[3] J. Hodge, “What is the difference between a conventional Radar and the SAR?” Website, May 2015. [Online]. Available: https://www.quora.com/What-is-the-difference-between-a-conventional-Radar-and-the-SAR?share=1

[4] M. Skolnik, *Radar Handbook*, 3rd ed. New York: McGraw-Hill, 2008.

[5] M. Mariotti d’Alessandro and S. Tebaldini, “Cross Sensor Simulation of Tomographic SAR Stacks,” *Remote Sensing*, vol. 11, p. 2099, 09 2019.

[6] E. Cherrington, Ed., *SAR Handbook: Comprehensive Methodologies for Forest Monitoring and Biomass Estimation*. SERVIR GLOBAL, SilvaCarbon, 2019. [Online]. Available: https://www.servirglobal.net/Global/Articles/Article/2674/sar-handbook-comprehensive-methodologies-for-forest-monitoring-and-biomass-estimation

[7] ESA ENVISAT, “The Advanced Synthetic Aperture Radar Guide,” Website, 2014. [Online]. Available: http://envisat.esa.int/handbooks/asar/CNTR1-1-2.html

[8] “Remote sensing tutorials,” Website, 2019. [Online]. Available: https://www.nrcan.gc.ca/maps-tools-publications/satellite-imagery-air-photos/tutorial-fundamentals-remote-sensing/9309

[9] *ICEYE SAR Product Guide*, 3rd ed., ICEYE, 2020. [Online]. Available: https://earth.esa.int/eogateway/documents/20142/37627/ICEYE-SAR-Product-Guide.pdf

[10] A. Moreira, “A Tutorial on Synthetic Aperture Radar,” *IEEE Geoscience and Remote Sensing Magazine*, March 2013.

[11] J. Fan, “Oil Spill Monitoring based on SAR Remote Sensing Imagery,” *Aquatic Procedia 3 - International Oil Spill Response Technical Seminar*, pp. 112 – 118, 2015.

[12] M. Skolnik, *Introduction to Radar Systems*, 2nd ed. New York: McGraw-Hill, 2001.

[13] T. Freeman, “What is Imaging Radar?” Website, NASA Jet Propulsion Laboratory. [Online]. Available: https://airsar.jpl.nasa.gov/documents/genairsar/radar.html

[14] L. J. Cutrona, *Radar Handbook*, 2nd ed. New York: McGraw-Hill, 1990, ch. Synthetic Aperture Radar.

[15] NASA Earthdata, “What is Synthetic Aperture Radar?” Website, Apr. 2020. [Online]. Available: https://earthdata.nasa.gov/learn/backgrounders/what-is-sar

[16] ESA, Earth Online, “Radar Course 3 - Image interpretation: Speckle,” Website, 2021. [Online]. Available: https://earth.esa.int/web/guest/missions/esa-operational-eo-missions/ers/instruments/sar/applications/radar-courses/content-3/-/asset_publisher/mQ9R7ZVkKg5P/content/radar-course-3-image-interpretation-tone

[17] AIRBUS, *TerraSAR-X Image Product Guide - Basic and Enhanced Radar Satellite Imagery*. [Online]. Available: https://www.intelligence-airbusds.com/files/pmedia/public/r459_9_20171004_tsxx-airbusds-ma-0009_tsx-productguide_i2.01.pdf

[18] ESA, “PolSARpro v6.0 (Biomass Edition) Toolbox Landing Page.” [Online]. Available: https://step.esa.int/main/toolboxes/polsarpro-v6-0-biomass-edition-toolbox/

[19] Alaska Satellite Facility, NASA, “ASF MapReady,” Website, 2021. [Online]. Available: https://asf.alaska.edu/how-to/data-tools/data-tools/

[20] L3HARRIS^{TM}, “ENVI® SARscape®,” Website, 2021. [Online]. Available: https://www.l3harrisgeospatial.com/Software-Technology/ENVI-SARscape

[21] BAE SYSTEMS, “Geospatial eXploitation Products™ (GXP®),” Website, 2021. [Online]. Available: https://www.baesystems.com/en/product/geospatial-exploitation-products

[22] C. Oliver and S. Quegan, *Understanding Synthetic Aperture Radar Images*. Scitech Publishing, Inc, 2004.

[23] NASA Earthdata, “Getting Ready for NISAR - and for Managing Big Data using the Commercial Cloud,” Website, 2020. [Online]. Available: https://earthdata.nasa.gov/learn/articles/tools-and-technology-articles/getting-ready-for-nisar

[24] F. Bordoni, M. Younis, N. Gebert, G. Krieger, and C. Fischer, “Performance Investigation on the High-Resolution Wide-Swath SAR System with Monostatic Architecture,” 06 2010, pp. 1122–1125.